OPERATION TANQUARY

GLACIER DEPTHS IN NORTHERN ELLESMERE ISLAND: AIRBORNE RADIO ECHO SOUNDING IN 1966

by

G. Hattersley-Smith, Anne Fuzesy and S. Evans

DEFENCE RESEARCH BOARD
DEPARTMENT OF NATIONAL DEFENCE
CANADA

DREO TECHNICAL NOTE NO. 69-6

Geophysics
Hazen 36

DECEMBER 1969
OTTAWA

DEFENCE RESEARCH BOARD

DEPARTMENT OF NATIONAL DEFENCE
CANADA

DEFENCE RESEARCH ESTABLISHMENT OTTAWA
GEOPHYSICS SECTION

GLACIER DEPTHS IN NORTHERN ELLESMERE ISLAND: AIRBORNE RADIO ECHO SOUNDING IN 1966

by

G. Hattersley-Smith
Defence Research Establishment Ottawa

Anne Fuzesy
and
S. Evans
Scott Polar Research Institute, Cambridge, England

DREO TECHNICAL NOTE NO. 69-6

Geophysics
Hazen 36

Published December 1969
OTTAWA

69-089

CONTENTS

	Page
Introduction	1
Apparatus	1
Navigational Methods and Plotting of Results	3
Routes and Flying Time	4
Antoinette Bay and d'Iberville Fiord Area	6
Flight of 16 April	6
Antoinette Glacier	6
Ice Cap	6
D'Iberville Glacier	7
Gilman Glacier, Mount Oxford Area, and Disraeli Glacier	7
Flight of 17 May	7
Gilman Glacier	7
Mount Oxford Area	8
Disraeli Glacier	8
M'Clintock Inlet, M'Clintock Glacier, Ice Cap, and Air Force Glacier	9
Flight of 17 April	9
M'Clintock Inlet	9
M'Clintock Glacier	10
Ice Cap	10
Air Force Glacier	10
Milne Fiord, Milne Glacier, Ice Cap, Henrietta Nesmith Glacier and Approaches	11
Flight of 19 April	11
Milne Fiord	11
Milne Glacier	11
Ice Cap	13
Henrietta Nesmith Glacier and Approaches	13
Otto Glacier, Ice Cap, Chapman and Bent Glaciers	13
Flights of 13 and 20 April	13
Otto Glacier	14
Ice Cap, Chapman and Bent Glaciers	15
Ice Caps South and East of Tanquary Fiord	16
Flight of 16 April	16
Results	16

Page

Ice Caps East of Hare Fiord 17
Flight of 20 April 17
Results 17

Ward Hunt Ice Shelf and Adjacent Coast 18
Results of 17 May Flight 18
Results of 19 May Flight 19
Discussion of Results 19

Summary and Conclusions 20

References 21

TABLE

Table I Flying programme for radio depth sounding in northern Ellesmere Island 5

FIGURES
(At end of report)

Fig. 1. Map of northern Ellesmere Island showing flight lines.

Fig. 2. Four-wire 35 Mc/s half-wave dipole antennas suspended beneath each wing of the Otter aircraft. Two of the conductors are driven from a coaxial cable which carries a ferrite-cored matching transformer at the centre. Conductors and supporting wires are assembled from 7/0.32 in., copperweld, "Nico-press" sleeves, and 1 in. egg insulators (all tested to 2,000 lb.).

Fig. 3. Otter aircraft with antennas rigged.

Fig. 4. Geometrical situation over Milne Glacier.

Fig. 5. Antoinette and d'Iberville Glaciers and adjoining ice cap: (a) flight line map, (b) profile, (c) film print to show subglacial ridge of Antoinette Glacier.*

Fig. 6. Gilman Glacier, Mount Oxford area and Disraeli Glacier: (a) flight line map, (b) profile, (c) film print of profile between terminus of Gilman Glacier and Mount Oxford,*(d) film print to show terminus of Disraeli Glacier.* The gap between Disraeli Glacier and the ice lobe to the north has widened since the map was made.

* See Note on page vi.

Fig. 7. Air photograph of lower Gilman Glacier from an altitude of 4,500 m, 2 August 1958. (Air photo RR 1511-15/16, by courtesy of National Air Photographic Library, Department of Energy, Mines and Resources).

Fig. 8. M'Clintock Inlet, M'Clintock Glacier, ice cap and Air Force Glacier: (a) flight line map, (b) profile, (c) film print to show terminus of M'Clintock Glacier.*

Fig. 9. Milne Glacier, ice cap and Henrietta Nesmith Glacier: (a) flight line map, (b) profile, (c) film print to show terminus of Milne Glacier,* (d) film print to show terminus of Henrietta Nesmith Glacier.*

Fig. 10. Air photographs of terminal part of Milne Glacier from an altitude of 10,000 m, 1959. Dashed line indicates approximate limits of grounding of the three ice tongues. (Air photos A 16728-14 of 28 July and A 16785-82/83 of 17 August, by courtesy of National Air Photographic Library, Department of Energy, Mines and Resources).

Fig. 11. Henrietta Nesmith Glacier and approaches: (a) flight line map, (b) profile.

Fig. 12. Otto Glacier, ice cap, and Bent Glacier: (a) flight line map, (b) profiles, (c) film print to show terminus of Otto Glacier.*

Fig. 13. Otto Glacier before the surge looking east from an altitude of 6,000 m, 15 July 1950. (Air photo T 405L-70, by courtesy of National Air Photographic Library, Department of Energy, Mines and Resources, Ottawa).

Fig. 14. Otto Glacier after the surge from an altitude of 10,000 m, 17 August 1959. (Air Photo A 16734-30 by courtesy of National Air Photographic Library, Department of Energy, Mines and Resources, Ottawa).

Fig. 15. Subglacial relief map of the terminal part of Otto Glacier, located by the four crosses which identify grid points 100/50, 100/175, 200/50 and 200/175 on the 1964 map of ice surface and rock relief (Faig, 1966). Control points marked on the contours result from four separate radio echo flight lines. Control is also established at glacier margins; exposed rock is stippled.

Fig. 16. Ice caps south and east of Tanquary Fiord: (a) flight line map, (b) profile.

Fig. 17. Air photograph of Hourglass Ice Cap from an altitude of 10,000 m, 29 July 1959. (Air Photo A 16693-34, by courtesy of National Air Photographic Library, Department of Energy, Mines and Resources).

---

* See Note on page vi.

Fig. 18. Ice caps east of Hare Fiord:
(a) flight line map, (b) profile.

Fig. 19. Ward Hunt Ice Shelf and adjacent coast:
(a) map showing spot ice depths, (b) film print of ice shelf and Cape Discovery ice rise (c) film print of Marvin ice rises* and adjoining ice shelf.*

* Note: A scale of metres depth is given at the ends of the print. This scale may be applied to echo delay times within the ice (vertical propagation is assumed). The horizontal scale is non-linear between the km marks and the features marked, which correspond to those on the map and profile.

GLACIER DEPTHS IN NORTHERN ELLESMERE ISLAND
AIRBORNE RADIO ECHO SOUNDING IN 1966

Introduction

In 1964 the Scott Polar Research Institute MK II very high-frequency radio echo apparatus was successfully used to sound the depth of the ice sheet in Greenland, providing a continuous profile of the bedrock surface by continuous recording from a moving surface vehicle (Bailey et al., 1964). The results of this work were mainly concerned with (1) a comparison with depths obtained by the seismic reflection shooting technique, (2) the relation between the radio echo strength and the ice temperature distribution, (3) the interpretation of reflecting layers discovered within the ice, and (4) the relation of the ice surface features to bedrock topography on the small scale (Robin et al., 1969).

The next step in the development of the apparatus was airborne testing, and in 1966 it was installed in a chartered DHC-3 Otter aircraft for flying operations based on Tanquary Camp, the Defence Research Board's field station in Northern Ellesmere Island. During the period 13-20 April, a number of flights were made over glaciers and ice caps in areas of Ellesmere Island north of lat 80° N. (Fig. 1), as reported briefly by Evans and Robin (1966). The present report analyses the results of these flights in detail.

Apparatus

Technical details of the S.P.R.I. Mark II radio echo apparatus, working on a frequency of 35 MHz, are given by Evans and Smith (1969), but several uncertainties were faced on this first airborne operation.

It was found difficult to choose a mounting position for the antennas so that they radiated mainly downwards, yet retained the broad-band impedance-matching characteristics necessary for the preservation of pulse shape and range accuracy, since this is invariably degraded in any radiator placed too close to a metal reflecting surface such as the aircraft skin. The radiators that were used are illustrated in Figs. 2 and 3. They were four-wire folded dipoles, designed and built by H. Serson at the Defence Research Telecommunications Establishment, and were rigged between the undercarriage fixing points and the wing tips on either side of the aircraft. No discernible effect of increased drag on the performance of the aircraft resulted. With this arrangement, it was found more satisfactory to use one antenna for transmitting and the other for receiving, rather than to use a single antenna for transmitting and receiving; the coupling between the two was measured to be -45 dB. These antennas represented an electrical and mechanical compromise excellent for a first trial, but there was a significant loss of range resolution and accuracy, and some loss of sensitivity, in this system and efforts to find better arrangements should be maintained. Most recently it has been found

that a folded dipole, 6 m long and terminated in an 800-ohm load resistor, may be rigged between the under-fuselage and pylons, 1 m long, on the wings of a DHC-3 Otter with very much better results.

A second uncertainty of this first airborne operation lay in the range of angles to the perpendicular from which echoes would be received after reflection at the top surface of the ice. When the flying height is too great, the oblique echoes from a rough surface, which scatters into a wide range of angles, may overlap in range with the perpendicular echo from the ice bottom. This is one factor, not in practice found to be very serious, influencing the choice of flying altitude. Oblique echoes from nunataks or valley walls need special consideration; they proved troublesome on several occasions in 1966. Quite frequently, echoes from small and isolated features of the landscape may be recognized by their change in range as the observer moves and by their tendency to form hyperbolic loci on a range/time record. Even if they are recognized, they may still obliterate the bottom echo.

A third uncertainty was the extent to which interference from other radio apparatus, particularly long-range transmitters, might interfere with reception. This was a consideration in the original choice of radio frequency; some problems of interference had already been experienced on the ground in 1964, and they were expected to be much more serious in the air. In 1966, in Ellesmere Island, this was not the case, but the situation might be quite different close to transmitting stations or at other phases of the sunspot cycle. Interference could be reduced but not eliminated by increasing the radio frequency; there would still be cross-modulation noise and strong interfering signals would generate their own harmonics and difference frequencies.

A final matter of concern was the relative strength of the top and bottom echoes. The situation in Ellesmere Island may be illustrated thus. At 1000 m above the surface, the echo from sea ice was about 80 dB over receiver noise (this provides direct confirmation of the overall system performance), from land about 70 dB, and from the top of a glacier of the order of 60 dB over receiver noise. Thus the glacier surface has a reflection coefficient of about -20 dB. The echo from the bottom of the glacier was almost always weaker by 10 or 20 dB, and this is the order of magnitude of the attenuation due to dielectric absorption in the ice under the prevailing conditions. Thus the bottom surface of the glacier has a reflection coefficient comparable with that of the top surface. It is possible to find exceptions to any of these statements, which are offered only as a guide and to show that in Ellesmere Island the difference in strength between top and bottom echoes did not constitute a serious problem. This was because the ice thicknesses were not great and the temperature nowhere near the melting point. Subsequently and in different glaciological situations, there has been a serious problem, the solution of which lies in improved receiver design.

A modified Mark II apparatus, working on a frequency of 110 MHz, was carried on one flight only. For this it was necessary to change components in the transmitter and receiver, and in particular to rig a different antenna. A rigid tubular folded dipole, also designed and built by H. Serson, was clamped on the wing strut, facing fore and aft, for the flight of 20 April.

The attraction of using a higher radio frequency lies in the possibility of reducing the antenna beam width, thus minimizing interference from features to either side of the line of flight. At higher frequencies it is also possible to improve the range resolution of both the antenna and electronic system. Disappointing results with the modified apparatus were due to reduced system performance, and no firm conclusion should be drawn about increased radio-wave absorption in ice at the higher frequency. It will become evident from the results in this report that over valley glaciers the overwhelming need is for a beam width of 15 degrees to the 3 dB points and down at least 25 dB at 45 degrees to the vertical.

Navigational Methods and Plotting of Results

Navigation was limited to line-of-sight paths or sun-compass courses from identifiable landmarks on air-photo mosaics. It was the practice at frequent intervals to record the aircraft aneroid altimeter reading, from which the true elevation of the aircraft above sea-level could be derived with an error less than ± 50 m. The cruising speed was 50 m/sec (100 knots) and a height of about 500 m above the ice surface was convenient. The flight lines have been plotted on the National Topographic System 1:250,000 maps, published by the Surveys and Mapping Branch, Department of Energy, Mines and Resources, Ottawa. The surface elevations on the profiles in this report have been taken directly from the maps by interpolation between the contours, and have been plotted here with a vertical exaggeration of 12.5 over the horizontal scale. The error in surface elevation will not exceed 60 m on the inland ice caps, and is considered to be much less in fiord areas. For correlation with the maps, the horizontal scale is given in kilometres from an arbitrary zero on the flight line.

Except for calculation of the range of oblique echoes, no use has been made of the aircraft altitude according to the aneroid barometer, nor of the known height of the aircraft above the ice surface, given by the delay of the surface echo. The radio-echo profiles of ice thickness are based on the difference in the echo time from the surface and from the bottom. This time difference has been converted to equivalent ice depth by using a velocity of propagation of 169 m/microsecond, even when there is a possibility that an echo arriving later than that from the ice surface may be an oblique reflection along a path entirely in air, for which the velocity of propagation would be 300 m/microsecond.

The time for the total sweep width on the cathode ray tube was 20 microseconds occupying 24 mm width on the film record. Positions could be measured to an accuracy of 0.1 mm, giving an uncertainty in depth measurement of about 8 m. A faster time sweep was used only on the Ward Hunt Ice Shelf (although it could have been more widely used), and for most of this area the random error is ± 4 m in ice depth.

A fuller discussion of the accuracy of radio echo sounding is given by Robin et al (1969), and it is appropriate here to discuss only the gross error of interpretation that can arise with oblique echoes. The echo from

an isolated reflecting facet, such as a nunatak, can usually be recognized by its range-time variation and slow fading rate. But an echo that may come from a valley wall requires more careful examination. Fig. 4 illustrates a specific geometrical situation encountered over the Milne Glacier between the 36 and 40 km marks (Fig. 9), where it was decided to examine if an echo apparently from an internal reflecting layer in the glacier was in fact a reflection from the valley wall. The true height of the aircraft above the glacier surface was known to be 1200 m from the delay time of the surface echo. The additional delay of the echo in question was 1.0 microseconds. With a velocity of propagation of 169 m/microsecond in ice and of 300 m/microsecond in air, the echo may have come from a reflecting layer in the ice 85 m vertically below the surface, or it may have come from a point X at a range 150 m greater than AS (Fig. 4) if the wave travelled wholly in air. In the latter case, the distance SX is 620 m. But the Milne Glacier is 4 km wide in this area, and the flight line was plotted up the centre. The error in plotting could not be so large that the aircraft actually passed 620 m from the bottom of one wall of the valley, and it is therefore concluded that the echo did in fact come from a reflecting layer within the ice.

Routes and Flying Time

During the period 13-20 April, radio echo sounding flights were made on six days, and a total of 18.3 hours were flown for a flying cost of $2,745 at $150/hour. Dates, times and routes of flights are shown in Fig.1 and Table I.

Fair to excellent radio echo records were obtained on these flights except in the following cases. On the 14 April flight, weather severely restricted the flying height, and only limited tests of the radio echo apparatus were possible. On the 19 April flight, no records were obtained over the Turnabout Glacier, Grant Ice Cap and Eugene Glacier owing to failure of the recording camera. Finally, on the 20 April flight, when the 110 MHz system was used for the only time during the flight series, no records were obtained over the eastern approaches and summit of the ice cap west of Tanquary Camp, although a valuable line of soundings was obtained on the Otto Glacier.

TABLE I FLYING PROGRAMME

Date and Time	Route	Flying Time (hr)
April 13 0930-1230	Eureka to Tanquary Camp *via* the Blackwelder Mountains, Mount Schuchert, Otto Glacier, ice cap, and Bent Glacier.	3
April 14 1700-1820	Tanquary Camp to Lake Hazen and return.	1.4
April 16 1800-2110	Tanquary Camp to Mer de Glace Agassiz and return *via* ice caps southeast of Tanquary Fiord, Antoinette Glacier, ice cap, d'Iberville Glacier, Viking and Ad Astra ice caps.	3.2
April 17 1530-2220	Tanquary Camp to Ward Hunt Island and return *via* Lake Hazen, Gilman Glacier, ice cap Disraeli Glacier, Ward Hunt Ice Shelf and ice rises, Cape Discovery ice rise, M'Clintock Inlet, M'Clintock Glacier, ice cap, and Air Force Glacier.	4.8 (not incl. 2 hr on ground at Ward Hunt Island)
April 19-20 1650-0100	Tanquary Camp to Alert and return *via* Air Force and Henrietta Nesmith glaciers, Lake Hazen, Turnabout Glacier, Grant Ice Cap, Eugene Glacier, Ward Hunt Ice Shelf, Cape Discovery ice rise, Milne Glacier, ice cap, Henrietta Nesmith Glacier, and Ad Astra Ice Cap.	3.7 (not incl. 2.5 hr on ground at Alert)
April 20 1740-1950	Tanquary Camp to Eureka *via* northwest valley, Yelverton Lake, ice cap, Otto Glacier, Mount Schuchert, and the Blackwelder Mountains.	2.2

Antoinette Bay and d'Iberville Fiord Area

Flight of 16 April

The flight (Fig. 5a) passed southward from Tanquary Camp to Antoinette Bay, thence up the Antoinette Glacier and across the ice cap to the head of d'Iberville Fiord. A return pass was made over the d'Iberville Glacier almost to its head, and the aircraft then returned via the small ice caps south and east of Tanquary Fiord to Tanquary Camp. The radar records are difficult to interpret, since there are few reliable bottom echoes and a good deal of interference from oblique echoes.

Antoinette Glacier

The floating tongue of the Antoinette Glacier is not sharply defined on the profile (Fig. 5b) because of numerous icebergs calving from a very active and broken ice front. The icebergs returned radar echoes indicating thicknesses up to 100 m or more. North of the 2 km mark the glacier is afloat, and at this point the thickness is 125 m. From the 7.5 km mark where the ice depth is 230 m, the bedrock appears to rise gradually from 80 m below to 100 m or more above sea level at the 14 km mark, where the ice depth appears to be about 280 m. The possible significance of such a subglacial ridge (Fig. 5c) is mentioned in the discussion on the Otto Glacier. There is apparently an internal echo from some feature at a depth of about 180 m between 9.5 and 12 km. Southward from the 14 km mark, the subglacial surface falls away while the ice depth increases, until at 25 km the ice is about 660 m deep and resting on bedrock near sea level. The glacier bed then appears to rise much more steeply than the glacier surface, although interference from oblique echoes makes it very difficult to interpret this part of the radar record. At the 30 km mark, the aircraft circled before turning west to avoid cloud; here the ice is probably about 400 m deep. The westerly tributary of the glacier was crossed near the 48 km mark, where the radar record indicates a trough with depths to 500 m.

Ice Cap

For the ice cap between the head of the Antoinette Glacier and the head of d'Iberville Fiord, the profile (Fig. 5b) shows very irregular bottom topography, with much interference from oblique echoes; ice depths probably do not exceed 300 m. An echo from an internal reflecting layer at a depth of 10 to 25 m, between the 57 and 63.5 km marks, provides the main interest of the record. Echoes arising from internal layers have been studied in detail in Greenland (Robin et al., 1969) and have been detected over wide areas of Antarctica (Polar Record, 1968). It is suggested that they may originate as sedimentary layers of slightly different density from that of the firn or ice immediately above and below. Work on the ice cap at the head of the Gilman Glacier at an elevation of 1800 m above sea level has shown clearly that ice layers are thicker and more numerous in the upper 13 m of firn than at depths of 13 to 39 m owing to generally warmer summers since about 1926 (Hattersley-Smith, 1963a). The elevation of the present internal reflecting layer ranges from 1100 to 1400 m above sea leavel, while the equilibrium line in this area probably lies between 1000 and 1200 m elevation. Accumulation is estimated to be of the order of 0.2 m H_2O/yr,

which over a 40-year period would amount to 8 m H_2O, or perhaps as much as 14 m of firn and iced firn. It therefore seems possible, with allowance for the uncertainty in accumulation in radar depth measurement, that the near-surface reflecting layer may be due to an increase in density of accumulating firn about 40 years ago, when the area entered a period of somewhat warmer summers.

D'Iberville Glacier

Over the d'Iberville Glacier bottom echoes from an ice depth of 600 m indicate that the ice is grounded 100 m below sea level as far as 15 km from the terminus (Fig. 5b). The glacier bed then rises rather steeply, so that at a distance of 20 km from the terminus the ice depth is only 350 m. From this point up-glacier oblique echoes make interpretation impossible, except at the 132 km mark, near the top of a tributary glacier from the west, where unambiguous bottom echoes indicate ice depths of 750 to 800 m. The return flight down the glacier added no further information, and the radar record has not been plotted.

Gilman Glacier, Mount Oxford Area and Disraeli Glacier

Flight of 17 May

The flight (Fig 6a) passed northward up the Gilman Glacier, thence westward over the ice cap to the divide near Mount Oxford. A return pass was made over the area from 10 km west to 15 km east of Mount Oxford, so that three radar profiles are available for this part of the traverse. The flight continued northward and north-eastward down the Disraeli Glacier to Ward Hunt Island, where a landing was made.

Gilman Glacier

The lower 12 km of the Gilman Glacier has an average width of 5 km and a rather regular bottom surface. These features make it ideally suitable for radio echo sounding, because they obviate interference from oblique echoes due to nunataks and side walls and from overlapping echoes due to irregular bedrock topography. Previous seismic and gravity profiling of the glacier (Weber, 1961 ; Weber et al., 1961) allow a comparison of results by these methods with the radio echo results. Agreement is very good, except that the seismic and gravity profile appears much smoother. Since seismic and gravity stations were on average 1 km apart, whereas the radar results have been plotted at 200 m intervals with the continuous record available for interpolation where necessary, the radar profile (Fig. 6b) undoubtedly gives a truer representation of the bedrock. With allowance for the vertical scale exaggeration of 12.5, the bedrock surface is seen to be slightly undulating. The direct print of the radio echo record (Fig. 6c) gives a true indication of the smallest directly detectable feature in the bedrock, but it is possible to derive statistical information about features smaller than those individually detectable. The greatest directly recorded slope of 9 degrees is in reverse direction to the slope of the top surface of the glacier and is evidently caused by the subglacial continuation of a

rock ridge on the west side of the glacier near the 8 km mark. At the surface this ridge is responsible for steepening slope leading to a depression (Fig. 7).

On the upper part of the glacier, from the 24 km mark westward, the radar profile shows sharp rises in the apparent bottom echo. However, the "tails" on the radar traces (passing below the previous clear bottom echo) and their steep hyperbolic and symmetric form suggest that they represent oblique echoes. The continuation of a clear bottom echo between the 35 and 40 km marks, indicating a gently sloping bedrock surface, also suggests that the break is due to oblique interference. However, it is not clear why the true bottom echo should be interrupted even when the presence of oblique echoes is accepted. Results of seismic and gravity depth-sounding over a 3 km long, northeast-southeast section of the upper Gilman Glacier near the 28 km mark show a wide and flattened U-shaped profile with a maximum depth of 830 m, decreasing to about 500 m near the sides (Weber, 1961). There is little doubt that this trough continues into the valley of the lower Gilman Glacier, for measurements by Arnold (Weber et al., 1961) showed that the glacier movement (15 m/yr) in the area of seismic and gravity sounding is directed approximately west-east towards the head of the lower glacier, where the movement is approximately the same (18 m/yr). At the 35 km mark, above the area of interference from oblique echoes, the radar results show ice depths of 800 m, agreeing closely with Weber's seismic and gravity measurements.

Mount Oxford Area

Between the 40 km mark and Mount Oxford the irregular character of the radar traces indicates very undulating subglacial topography as well as considerable interference from nunataks and thinly covered lateral ridges. On two of the passes the echo from Mount Oxford "breaks the surface", although the routes were plotted 1 to 2 km south of the mountain. This effect, clearly seen in the radar record (Fig. 6c), means that some part of the mountain face was at a lesser range than the smooth ice surface vertically below the aircraft. The radar results give average maximum depths of 400 m for the ice near Mount Oxford in agreement with Weber's results from seismic reflection shots.

Disraeli Glacier

A rock ridge, running westward from Mount Oxford and exposing several nunataks, divides the névé to south and west from the uppermost reaches of the Disraeli Glacier. The profile (Fig. 6b) shows ice depths up to 500 m, and also shows the rock ridge "breaking the surface", then falling away steeply to the Disraeli Glacier in the pass that lies between Mount Oxford and the ice cap to the west. At the bottom of this pass, near the 66 km mark, there is much interference from oblique echoes which prevents detection of a bottom echo. The glacier leaves the pass through a narrow rift in a second east-west rock ridge, where crevassing indicates steepening bedrock and ice that is probably of no great depth. For the wide glacier basin below the crevassed area, between the 70 and 72 km marks, good bottom echoes were obtained from a depth of 650 m. But from 72 to 76 km there is a remark-

able shallowing of the ice in an area where a small nunatak is visible in the air photographs, and it is concluded that, beneath the high flat central part of the basin, the bedrock rises to within 200 m of the surface probably over a wide area, as suggested by the surface contours on the 1:250,000 map (Fig. 6a).

Between 79 and 81 km characteristic bottom echoes are again seen from a depth of 650 m, but there is some overlapping with oblique echoes where the glacier enters its valley proper, which has a width of only 3 km. At the 83 km mark, where the valley widens to 4 km, the bottom echo returns clearly from a depth of 500 m. At 90.5 km the valley narrows abruptly to a width of 2 km between very steep walls and the bottom echo is completely obliterated by oblique echoes that continue to the 108 km mark, where the glacier widens again to 3 km. From 108 to 121 km the bottom echo reappears at depths ranging from 550 to 350 m. Over the terminal 9 km stretch of the glacier, the record (Fig. 6d) as far as the 125 km mark is again difficult to interpret because of oblique echoes. The glacier is probably grounded below sea level from the 121 to the 126.5 km mark where it floats off at an ice thickness of about 120 m; the boundary between the grounded and floating part of the glacier is clearly seen on the radar trace from the change in surface slope and the sudden increase in echo strength by about 10 dB. The floating tongue is 1.25 km long, and the ice front is separated by a 1.5 km expanse of fiord ice from the floating ice lobe shown to the north on the 1:250,000 map (Fig. 6a). It is not possible to distinguish separate top and bottom echoes from the thin, probably freshwater ice of the fiord, but good bottom echoes from the ice lobe give a maximum thickness of 90 m. The latter feature was sounded for 10 km of its 14 km length before the film ran out. It appears to have been formed by a large and very active glacier from the southeast and by a smaller feeder from the northeast pushing out and expanding into a composite lobe along the line of the fiord.

M'Clintock Inlet, M'Clintock Glacier, Ice Cap and Air Force Glacier

Flight of 17 April

The flight passed from Ward Hunt Island westward to Cape Discovery, up M'Clintock Inlet and the length of the M'Clintock Glacier, across the ice cap and down the Air Force Glacier to Tanquary Fiord (Fig. 8a).

M'Clintock Inlet

Air photographs of June 1962 show the outer 15 km of M'Clintock Inlet covered by unbroken ice shelf. On the present flight, the M'Clintock Ice Shelf was seen to have disintegrated to leave scattered, disoriented fragments (or small ice islands), except over an area of about 10 km^2 around Borup Point and in the embayment north of Cape Discovery, where parts of the ice shelf precariously remain (Hattersley-Smith, 1967). It is evident that after fragmentation, most of the ice shelf in the inlet moved out to sea. As a result of this break-up, no ice shelf appears on the radar records for the inlet, except off Cape Discovery (Fig. 19a).

M'Clintock Glacier

The small island, 3 km north of the ice front of the M'Clintock Glacier, provided a useful check point for the start of the radio sounding record (Fig. 8b). The glacier is afloat in its lower 10 km (Fig. 8c) and the boundary between the floating and grounded ice is easily distinguished in air photographs. Decrease in strength of the bottom echo and the rise of the surface echo show that the point of grounding is near the 13 km mark. Thickness ranges from 25 to 50 m for the floating ice tongue, and the glacier increases rapidly in thickness from 50 m at the point of grounding to 150 m at the 17 km mark and 500 m at the 28 km mark, where good bottom echoes were obtained. Between 18 and 22 km there is considerable interference from oblique echoes, which is not surprising because the valley over this stretch of the glacier is less than 1.5 km wide and very steep-sided. Maximum over-deepening is evident at 28 km, beyond which reliable bottom echoes show a rising valley floor. Although the valley widens gradually to 2-3 km near the 38 km mark, there is still interference from oblique echoes, but fortunately not enough to obscure the bottom echo. It is of interest to find that the valley floor continues below sea level to the 38 km mark, where the ice is 580 m thick. As in the case of the Milne Glacier, the subglacial profile indicates either very much more extensive drowning of the preglacial valley than might be suspected from the map, or considerable erosion and over deepening by the glaciers (Hattersley-Smith, 1969). The form of the valley floor, rising gradually from the 28 km mark to the snout of the M'Clintock Glacier, is suggestive of considerable quantities of morainal material being deposited or pushed out at the glacier terminus.

From 38 km the glacier appears to maintain a thickness of about 600 m as far as the 47 km mark, where it broadens into an extensive basin that receives tributary glaciers from east and west. Good bottom echoes over this area show a gently undulating subglacial surface with ice thicknesses up to 620 m. Beyond the 53.5 km mark the bottom echo is lost within echoes coming from the west wall and from nunataks and buried rock ridges at the head of the M'Clintock Glacier.

Ice Cap

Between 71.5 and 76 km good bottom echoes indicate ice depths up to 900 m on the ice cap at the head of the Air Force Glacier. These ice depths, which are the greatest so far recorded from northern Ellesmere Island, mean that the bedrock at the divide between the M'Clintock and Air Force glaciers is at an elevation of only 650 m above sea level. Only 10 km southeast of the divide,a mountain ridge rises to an elevation of about 2400 m. This gives some idea of the very considerable bedrock relief in the area, and points to the essentially mountain character of the glaciation that affected a landscape already deeply dissected by river erosion (Hattersley-Smith,1969).

Air Force Glacier

Ice depths on the Air Force Glacier range from 680 m at the 86.5 km mark to 240 m within 2 km of the snout; the glacier thins rapidly in the final 2 km. Between 86.5 and 105 km the bedrock surface is undulating with

an average slope of less than 1 degree. Ice depth decreases gradually to 400 m at 103 km and then abruptly to 300 m at 105 km. At this point the valley of the glacier narrows from 5 km to 3.5 km in width, and the slope of the bedrock steepens to 3.5 degrees. This slope is maintained as far as the 111.5 km mark, where the elevation of the bedrock is only 20 m above sea level. From 111.5 to 114 km the bedrock rises to 110 m then falls to 70 m above sea level in the terminal 0.5 km of the glacier. The most probable explanation of the form of the bedrock profile is that the glacier has pushed up and advanced over moraines and outwash material near its terminus. Certainly the glacier has been advancing during the last 900 years, as shown by the radiocarbon age of organic material in varved silts exposed a short distance from the snout (Hattersley-Smith, 1969). Radar echoes off the snout of the glacier are demonstrably due to oblique echoes from the steep valley walls.

Milne Fiord, Milne Glacier, Ice Cap, Henrietta Nesmith Glacier and Approaches

Flight of 19 April

The flight passed from Tanquary Fiord up an unnamed glacier leading to the head of the Henrietta Nesmith Glacier, and then down the latter glacier. The flight was continued to Alert, thence westward along the north coast of the island, passing over the Ward Hunt Ice Shelf and associated ice rises, up Milne Fiord and the length of the Milne Glacier, across the ice cap and again down the Henrietta Nesmith Glacier (Fig. 9a).

Milne Fiord

Milne Fiord is the only fiord of northern Ellesmere Island where the main outlet glacier is contiguous with ice shelf; this has been the case at least since 1948 when the first air photographs of the area were taken. The fiord is completely filled by ice shelf from the ice front to the outer coast, and the boundary between ice shelf and glacier is approximately as shown on the map (Fig.9a). Unfortunately, the ice shelf was not picked up on the radar trace, since the recording camera was not working until the aircraft was over the glacier. Air photographs (Fig. 10) show that, for a distance of about 3 km from the ice front, the ice shelf is more corrugated and appears to be thicker than immediately to the northwest, possibly because of pressure from the glacier and inclusion in the ice shelf of icebergs from the glacier.

Milne Glacier

The very confused surface appearance of the glacier is due to its formation from three merging ice tongues. The central tongue comes from the main valley leading to the highest accumulation areas of the ice cap, while the other two come from tributary glaciers on the southwest and northeast sides, joining the main glacier at distances respectively of 10 and 19 km from the ice front (Fig. 10). The central and northeastern ice tongues are clearly afloat at their northeastern margins, for they calve into a marginal lake at sea level, but from inspection of air photographs the proportions of them afloat are uncertain. The southwestern ice tongue appears to go afloat

a short distance below the icefall near shore.

Although the radar record does not show any recognizable transition from ice shelf to glacier, it does show at the 3.5 km mark a surface step and an increase in ice thickness from 60 to 130 m (Fig. 9 b,c). This is interpreted as marking the transition from the southwestern to the central ice tongue with its greater surface relief and thickness. Then, at the 6 km mark on the record, there is a sharp reduction in ice thickness to 20 m, corresponding to lake ice in a gap between two ice tongues, clearly visible in the air photograph (Fig. 10). The radar record then returns to the central ice tongue, and ice thickness increases to 120 m. At the 11.5 km mark a sharp decrease in bottom echo strength is interpreted as marking the change from floating to grounded ice. It seems likely that the glacier is grounded on an old terminal moraine with submarine relief up to 100 m. At a distance of 2-3 km down-glacier from the area of grounding, a transverse melt stream is an unusual surface feature that is believed to be controlled by the line of a hinge crack. Certainly the ice surface becomes much rougher below this melt stream, and this roughness may well have been initiated by crevassing during rapid movement afloat. The central ice tongue now appears to be relatively inactive, and is in any case partly impounded against the northeast side of the fiord by the more active southwestern tongue pushing over. This displacement to the northeast provides confirmation of the extent to which the central ice tongue is afloat. Air photographs of 1950 and 1959 show that the position of the ice front has changed little in the 9-year period; they indicate a rate of surface movement of about 10 m/yr, an amount that could easily be balanced by melting and calving at the ice front. If there is net thinning of the central ice tongue at the present time, new hinge lines could be expected to develop, and two such appear to be forming in the apparent area of grounding. On the northeastern ice tongue a transverse melt stream may also have formed along the line of a hinge crack, and thus may mark the area of grounding. The approximate limits of grounding of the three ice tongues are shown in Fig. 10. For the composite terminal area of the Milne Glacier radio echo sounding has provided the essential clues for determining the approximate limits of grounding of the three ice tongues.

Continuing up the glacier, the radar trace shows the ice thickening to 280 m at the 15 km mark, whence to the 45 km mark generally good bottom echoes indiate that the glacier is grounded below sea level with ice depths increasing from 280 to 740 m. Oblique echoes, causing interference between 26 and 31 km and at about 45 km, can be shown to come from nunataks readily identifiable in the air photographs.

Between 36 and 41 km, echoes were received from an internal reflecting layer at a depth that decreased in the up-glacier direction from 200 to 80 m; the geometry of the situation precludes the possibility of an oblique echo, as already discussed. The layer has an attitude of about 2 degrees to the horizontal and dips into the glacier at an angle of about 1 degree. Internal reflecting layers previously described (Robin et al., 1969) could be shown on acceptable assumptions to represent the top surfaces of former times, but in the present case the surface of the glacier above the reflecting layer is at an elevation of less than 500 m in an area where the equilibrium line is believed to lie at an elevation of 1000 m or more. It is difficult to see

how the layer could have originated as a surface layer of firn that underwent abnormal diagenesis due, say, to exceptional summer melt, because a particular sedimentary layer should occur at progressively greater depths up-glacier, not at shallower depths as here. The possibility that the layer is caused by internal fracture or shearing cannot be excluded.

From 45 to 65 km there is considerable interference from oblique echoes due to nunataks and thinly covered rock ridges, but the broken line of bottom echoes can still be identified on the radar trace. South of the 45 km mark the bedrock surface rises more steeply from sea level as the ice depths shallow from 740 m to 400 m or less.

Ice Cap

Between the heads of the Milne and M'Clintock glaciers the radar record is blank, but an oblique echo is picked up from a nunatak at the head of the latter glacier. Between the M'Clintock Glacier and Henrietta Nesmith Glaciers, it is evident from the undulating surface topography of the ice cap that the bedrock is very irregular. From the 105 to 108 km mark, in an area where oblique echoes can be excluded, it is seen from the radar trace that the bedrock rises almost to the surface. However, a little further to the east, at the 113 km mark, the flight passed near the north side of the high mountain ridge, so that irregular reflections here are probably due to oblique echoes. From 115 to 120 km good bottom echoes were obtained from depths of 480 to 280 m.

Henrietta Nesmith Glacier and Approaches

At the head of the Henrietta Nesmith Glacier on passage from the Milne Glacier, oblique echoes almost completely obscure the bottom, although this may be identified at a depth of 400 m at the 127 km mark. From 131 to 152.5 km excellent bottom echoes were obtained at depths varying from 580 to 680 m; the glacier then begins to shallow towards the snout and the surface slope steepens. At 154 and 157 m there are two distinct subglacial ridges, rising to 80 and 100 m above the glacier bed (Fig. 9b, d); these may well be terminal moraines that have been overridden by the ice, since it is well established that the major glaciers of the area have been advancing during the last 1,000 years or more (Hattersley-Smith, 1969).

On the approach to the Henrietta Nesmith Glacier on the outward leg of the flight, from the direction of Ekblaw Lake, the radar record (Fig. 11a) illustrates well the effects of oblique echoes and rugged subglacial topography for the glacier running northeastward from the west end of the lake; ice depths up to 460 m were recorded (Fig. 11b). The profile of the Henrietta Nesmith Glacier on this part of the flight, although less complete, is in good agreement with the later profile (Fig. 9b).

Otto Glacier, Ice Cap, Chapman and Bent Glaciers

Flights of 13 and 20 April

The flight of 13 April passed northward from Eureka to cross Hare and

Otto fiords near the Van Hauen Pass. The aircraft then flew up the Otto Glacier to its head, turned and made a return pass over the length of the glacier, before continuing east over the ice cap and southeast down the Bent Glacier to Tanquary Camp (Fig. 12a). The 20 April flight passed northeastward from Tanquary Camp to Yelverton Lake, thence westward over the ice cap and down the Otto Glacier. As a result of the two flights, radar ice-depth profiles are available on four lines spaced about 0.5 km apart over the length of the Otto Glacier, and on a line across the ice cap between the Otto and Bent glaciers. On the Bent Glacier and on the glaciers leading up to the ice cap from Yelverton Lake few data were recorded.

Otto Glacier

The Otto Glacier is a rare case of a high Arctic glacier that is known to have surged. The discovery was made from observations on a flight over the glacier in July 1963 (Hattersley-Smith, 1964). It was observed that in its lower 25 km the surface of the glacier showed the intense crevassing of a fast-moving ice stream, in contrast to the smooth appearance of the great majority of the main outlet glaciers in the area. Subsequent examination of three sets of air photographs taken in July 1950 (Fig. 13), July 1959 and August 1959 (Fig. 14) showed a very remarkable change both in the surface and in the terminal extent of the glacier in the period of nine years. All the crevassing had occurred during this period, all the surface melt streams so typical of glaciers of this region in summer had been obliterated, and stagnant ice had been overridden. The terminus of the glacier, grounded below sea level in 1950, had by 1959 advanced about 3 km as a floating tongue with calving of many icebergs. The glacier was rephotographed from the air in 1964, and maps were prepared at the scale of 1:50,000 from the 1959 and 1964 photographs of the lower 15 km of the glacier (Faig, 1966; Konecny, 1966). A further advance of the floating ice front, between 1959 and 1964, of 2-3 km was measured, and the horizontal movement during a period of 41 days in July-August 1959 was calculated as a maximum of 317 m(7.7 m/day) for the Otto Glacier. In the same period the maximum movement of its main tributary on the south side was calculated as only 34 m (0.83 m/day). In the part of the glacier that was mapped, there was no volume change; the lower 15 km was seen to have slumped and moved forward. In the height zones from 0 to 250 m above sea level the mean height change in the surface of the glacier ranged from +40.4 m in the 0 - 50 m zone to -26.1 m in the 200 - 250 m zone, which was equivalent to a mean height change below the 250 m level of -3.93 m or -0.79 m/yr. The mean height change over the whole glacier for the same 5-yr period was +1 mm/yr.

The records from the four radio-sounding passes over the Otto Glacier are presented in a composite profile spaced across the glacier in a roughly south-north direction (Fig.12b). The ice depth data have been combined with the topographic data on the 1964 glacier map to derive a map of subglacial topography of the lower 15 km of the glacier (Fig. 15). In the case of the tributary glacier from the south the bedrock contours have been extrapolated from those on the bare rock ridges on either side. The bedrock contouring is of course continued only to where the glacier goes afloat,since no echoes are received through water. The points of grounding of the glacier tongue have been derived from the radio echo traces(e.g. Fig. 12c), and the surface ele-

vation of the floating ice has been estimated from the thickness on the assumption that the glacier is solid ice of specific gravity 0.92 in hydrostatic equilibrium in sea-water of salinity 30‰.

The profiles and the subglacial topographic map show a subglacial ridge extending halfway across the glacier and to more than 125 m above sea level. On the north side of the ridge, however, the glacier bed falls away to about 125 m below sea level over half the width of the valley. The crest of the ridge, which seems more likely due to a bedrock spur than to glacial deposits, is marked in the air photographs of 1950 and 1959 (Figs. 12 and 13) by a small melt-water lake lying between two ice streams, those of the main glacier to the north and of the tributary glacier to the south. The radar profile shows an ice thickness in this area of 70 m, the shallowest depth found on the lower part of the glacier. Before the surge the ice in this height zone was on average 26 m thicker (Konecny, 1966).

The cross-section of the glacier bed in the area of the subglacial ridge is seen to be roughly S-shaped with a maximum difference of relief of about 250 m. The glacier surface elevation does not reflect such changes in bottom relief, so that the ice on the north side is up to 250 m thicker than on the south side and may be expected to move with higher velocity. In fact, the flow lines of the glacier, evident in the air photographs, conform to the contours on the bedrock map. The surge had the effect of allowing the northern and deeper ice stream of the main glacier to push southward the stream from the tributary glacier. Robin (1969) notes that the subglacial ridge causes the ice to decrease rapidly in thickness downstream; he suggests that the situation could lead to a change from compressive to extending flow and to the development of stress instabilities capable of initiating a surge. Up-glacier from the ridge, where the glacier bed falls below sea level, the ice thickens from 300 to 700 m. From the 26 km mark, where the glacier bed is 100 to 200 m above sea level, heavy crevassing ceases; in this area the glacier bed is undulating with maximum slopes up to 8 degrees. Between the 29 and 33 km marks, there is general steepening of the glacier bed, which then levels off to give an appearance of overdeepening at the head of the glacier where ice depths of 400-600 m were recorded. At the head of the valley, bottom topography is very irregular, and nunataks and submerged rock ridges produce sudden rises in the bottom echo.

Ice Cap, Chapman and Bent Glaciers

Between the 47 and 70 km marks, the radar trace shows underlying mountainous terrain which is reflected in the undulating surface topography of the ice cap, ranging in thickness from 200 to 400 m. From the 70 km mark to the head of the Chapman Glacier, good bottom echoes show gradual deepening of the ice to 760 m in a subglacial through-valley between the Chapman Glacier and an unnamed glacier flowing towards Yelverton Inlet. The map contours and ice depths indicate a subglacial saddle at an elevation of 950 to 1000 m above sea level. The Chapman Glacier shows the following features indicative of a glacier that may have surged: a large area of stagnant, moraine-covered ice near the terminus; a contorted pattern of surface moraines; and irregular surface drainage and puddling. It may therefore be worth emphasizing that it drains a very deep ice basin through a compara-

tively narrow gap in a mountain rim. East of the head of Chapman Glacier the ice cap shallows gradually to 200 - 400 m over buried mountains.

Because of the very steep gradient of the valley, no identifiable bottom echoes were obtained over the Bent Glacier, except in the terminal 1.5 km where ice depths decreased from 125 to 60 m at the snout of the glacier.

Ice Caps South and East of Tanquary Fiord

Flight of 16 April

The unnamed ice cap, 10 km south of Tanquary Camp, was crossed from north to south on the outward leg of the flight from Tanquary Camp to the Antoinette Bay and d'Iberville Fiord area, and on the return leg the Hourglass and Viking Ice Caps were crossed on south-north lines and the unnamed ice cap on an east-west line. The flight lines are shown on the map (Fig. 16a).

Results

The profiles (Fig. 16b) of all three ice caps indicate very irregular bottom topography, as might be expected from the nature of the surrounding terrain. In the case of the Hourglass Ice Cap, overlapping echoes were recorded from up to three different surfaces, but it has been assumed that the shallower or shallowest echo gives the depth of ice beneath the aircraft and that the other echo or echoes are oblique from inclined subglacial surfaces. Between the 3 and 5 km marks, surface topography of the southern lobe of the ice cap is seen to reflect the subglacial topography, with ice depths ranging from 80 to 100 m. In the valley between the two lobes of the ice cap, ice depths up to 70 m are recorded in the narrow connecting neck of ice. The northern lobe of the ice cap is thinner on the south side - 50 to 70 m - than on the north, where ice depths up to 160 m were recorded. Except in the area of the small glacier tongue on the northwest side, the rate of movement of this ice cap must be very low. It is suggested, therefore, that the greater ice depth on the north side has been due almost entirely to higher net accumulation, and that this is controlled by wind action. With a maximum elevation of only 1220 m, there is little doubt that the ice cap has been thinning in recent decades, and indeed an air photograph of August 1959 (Fig. 17) shows the whole ice cap as an ablation area.

On the unnamed ice cap a change of echo strength at the 24 km mark gives the position of the ice edge and a useful check on the navigation. On the east-west profile, if overlapping echoes are ignored, ice depths are seen to range from 65 to 130 m, with depths up to 230 m over subglacial valleys. On the north-south profile, ice depths up to 200 or more were found. Like the Hourglass Ice Cap, this ice cap with a maximum elevation of only 1350 m has probably undergone a period of recent thinning, for the air photographs of August 1959 show the snowline at an elevation of at least 1250 m above sea level. A thin body of snowdrift ice, 7 km south of the ice cap, failed to leave any record on the radar trace.

The radar record from the Viking Ice Cap presents a rather confused picture of overlapping echoes, with ice depths up to 200 m. Near the summit, however, the record suggests bare or very thinly-covered rock.

Ice Caps East of Hare Fiord

Flight of 20 April

On this flight from Tanquary Camp to Eureka *via* the Otto Glacier, the route passed north-south over the ice cap northwest of Mount Schuchert and over the ice cap of the Blackwelder Mountains (Fig. 18a). The flight of 13 April northward from Eureka to Tanquary Camp *via* the Otto Glacier also passed over these ice caps, but the radio sounding records, which do not add significantly to those of April 20, have not been plotted.

Results

Although the radar record (Fig. 18b) does not show the northern edge of the ice cap northwest of Mount Schuchert, good bottom echoes between the 6 and 8.5 km marks indicate ice depths increasing from 60 to 250 m in a slight subglacial depression. Thence to the 12.5 km mark, near the crest of this part of the ice cap, the ice cover thins gradually to 175 m. The rising subglacial relief in this area conforms in general to the surface relief of the ice cap. At the crest of the ice cap, a second apparent bottom echo is recorded from a depth of 390 m. If both echoes are from the bottom, it is possible that the sudden increase in ice depth is due to a subglacial extension of the northeast-southwest valley that flanks the northwest side of the Blue Mountains, although contours at the head of the valley hardly support this hypothesis. The lower echo may well come obliquely from an inclined subglacial surface. Southeastward from the crest of the ice cap, the ice thins rapidly towards the ice-covered valley north of the Mount Schuchert Glaciers. Depths near the southeastern margin of the ice cap average from 30 to 50 m. The radar trace for the ice-covered valley shows a good deal of interference from oblique echoes, some perhaps from bare rock, but ice depths up to 140 m are likely.

The radar profile for the ice cap of the Blackwelder Mountains has been drawn on the best interpretation of uncertain flight times. The transition from rock to ice at the northern outlet glacier is not seen on the radar trace, but ice depths appear to range up to 250 m on this side of the ice cap, if an apparent oblique echo near the 4 km mark is ignored. With rising subglacial relief the ice thins to 80 m at the crest of the ice cap; it thickens to 110 m at the top of the southern slope, then thins again towards the southern margin, which is clearly visible on the radar profile.

Except for the glacier tongues, the area of the ice cap of the Blackwelder Mountains is largely circumscribed by the 2500-ft. (762 m) contour; the same is also true of the ice-covered area around Mount Schuchert and of the ice cap to the north. The generally greater ice depths on the northern and northwestern sides of these ice masses may be due in part to lower ablation on northern than on southern slopes, but perhaps more importantly to

greater accumulation on the northern slopes. The predominant winds in the outer part of Hare Fiord are known to come from the southeast (Hattersley-Smith and Serson, 1966), and these may well tend to dump snow on northern and northwestern slopes.

Ward Hunt Ice Shelf and Adjacent Coast

Radio echo sounding flights were made over this area on 17 and 19 April. Information was obtained on ice thicknesses of the Ward Hunt Ice Shelf, the Ward Hunt Ice rise, the Cape Discovery ice rise, the small ice rises north of the Marvin Islands, and of ice caps to the south of capes Columbia, Nares and Albert Edward. The data are presented in the form of spot depths on the map (Fig. 19a). The present extent of the Ward Hunt Ice Shelf is plotted from air photographs of June 1962 after the massive calving of the previous winter (Hattersley-Smith, 1963 b), since when there has been only minor crumbling of the ice front. The present limited extent of ice shelf in M'Clintock Inlet is roughly shown on the map from observations on the present flights.

Results of 17 May Flight

The outward route passed down Disraeli Fiord, over the southernmost of the Marvin Islands and two of the small ice rises to the north (where good visual fixes were obtained), thence in an east-west arc across the Ward Hunt ice rise, continuing in a circle around the south side of Ward Hunt Island for a landing on the island's small lake. On the return, after circling the Ward Hunt and Marvin ice rises, the aircraft headed westward to cross the Cape Discovery ice rise, thence southward up M'Clintock Inlet. There is some uncertainty in the courses taken on the flights around Ward Hunt Island, so that north and northwest of the Marvin ice rises spot depths have been plotted in estimated positions which take account of the aircraft flight time, the measured ice thickness, and other factors that may be judged from the radio echo records, viz: changes in surface elevation, and whether the ice appears to be grounded or floating. Thus, although the quality of the records is such that the depths can be considered reliable to $\pm$ 4 m, the positioning is unreliable.

Good radio echo returns were received from the ice-rock interface on two of the Marvin ice rises, and these are associated with recognizable rises in the surface echoes. Maximum ice depths of 50 and 85 m were indicated for the northern and southern ice rises respectively. Between the northern ice rise and the eastern end of the Ward Hunt ice rise, ice shelf depths ranged from 50 to 80 m. The Ward Hunt ice rise itself is distinguished from the shelf by the smooth surface echo, and ice depths ranged from 40 to 100 m on the east-west pass. On the return pass from Ward Hunt Island, the records confirmed the ice depths on the Marvin ice rises, but provided no information on ice shelf thicknesses because of obliteration of the shallow bottom echo by a strong surface echo. They gave additional data on the Ward Hunt ice rise, showing depths in the southern part of 45 - 55 m, and a good profile of the Cape Discovery ice rise, reproduced directly in Fig. 19b. Spot depths on the map for the latter feature are plotted from the 19 May records which

are closely comparable.

Results of 19 May Flight

The flight passed from east to west along part of the north coast of the island, the record starting at the glacier on the west side of Parr Bay. A few good bottom echoes from the northern margin of the Mount Hornby ice cap give a maximum ice depth of 135 m. The transition from land to ice shelf in Markham Fiord is well shown on the record, and two reliable ice depths of 20 and 25 m are available for the ice shelf in this fiord. A maximum depth of 140 m is shown for the ice cap southwest of Cape Nares, and of 170 m for the ice cap southeast of Cape Albert Edward.

Leaving Cape Albert Edward, the record shows a sharp step marking the transition from land to ice shelf, 20 to 25 m thick near shore (Fig. 19c). The ice rise, 5 km west of the cape, is clearly shown by a change in echo strength where the ice goes aground, the limit of grounding being the ice shelf boundary as plotted on the map (Fig. 19a). The ice rise has a maximum thickness of 40 m. Passing from this ice rise, the record again shows a clear transition from grounded to floating ice increasing in thickness from 25 to 40 m southwestward. Ice depths up to 20 and 35 m are recorded on the eastern and southern respectively of the Marvin ice rises. Only one reliable ice depth is recorded between the Marvin ice rises and Cape Discovery, namely 40 m off Cape Alexandra. The transition from ice shelf to grounded ice on the east side of the Cape Discovery ice rise is clearly seen, and there is a good record across the ice rise showing ice depths ranging from 50 to 125 m over a subglacial surface that reaches a maximum elevation of about 160 m above sea level. The record shows a clear transition from the ice rise to the ice shelf on the east side of M'Clintock Inlet where the ice depths for the shelf are 30 to 50 m, or appreciably less than on the adjacent ice rise.

Discussion of Results

From results at five seismic shot points, the greatest thickness of ice shelf found by Crary (1958) was 54 m at a point about 10 m southwest of Ward Hunt Island, where a level survey gave a surface elevation of 6.5 m. The seismic data of Crowley (1961) and the thermal and survey data of Lyons and Leavitt (1961) showed that the ice shelf varied in thickness from 20 m at its seaward edge to 47 m in the area between Ward Hunt Island and the mainland; a mean thickness of 43 m was indicated. The main interest in the radio sounding results lies in the ice depths between the Marvin ice rises and the Ward Hunt ice rise , which are greater than any previously recorded from the ice shelf or indeed from the ice island T-3 (Crary, 1958). They imply a surface elevation of the ice shelf in this area of 9.5 m, for which there is at present no confirmation from gound data. However, since the radio echo traces are good, there is no reason to reject the results, although some further comment may be in order.

Throughout this report, all ice depths have been calculated on the assumption that the velocity of propagation of radio waves in ice is 169 m/microsecond (Robin et al., 1969). No correction has been added for the lower density of firn near the surface allowing a higher velocity of propagation;

it is possible that this correction could amount to +10 m in the total depth, but only for the higher areas of the ice cap. In view of the surprisingly large apparent depths in one area of the ice shelf, it is necessary to enquire what effect liquid water or brine pockets may have in reducing the average wave velocity and thus increasing the echo delay time. It is fortunate that directly relevant values are available for the dielectric permittivity of ice cores taken from glacier ice zones and sea ice zones of the Ward Hunt Ice Shelf (Ragle et al., 1964). These show that the dielectric loss tangent in the sea ice zone is almost twenty times greater than in the glacier ice zone; in fact at -1°C it is estimated that, in the sea-ice zone, the absorption would be 120 dB/100 m in depth. Thus, any greater concentration of water, brine, or impurity, if it occurs, will make it almost impossible to detect echoes in ice 50 m or more in thickness. At the same time, the relative permittivity of the samples from the sea-ize zone averages 3.30 between 0° and -20°C, which is not significantly greater than the value for the glacier ice zone and only a little greater than the value used throughout the present reduction. In fact, it corresponds to a velocity of propagation of 165 m/ microsecond. Until any new evidence becomes available, ice depths from 50 to 80 m must be accepted for the ice shelf to the east of Ward Hunt Island.*

On the Ward Hunt ice rise, Lyons and Ragle (1962) recorded a depth of 52.25 m by coring to the bottom of the ice at a site 0.5 km from the shore of the moat on the north side of Ward Hunt Island. The radio sounding gave a maximum depth of 100 m for this ice rise and the range of depths may be judged from Fig. 19a. Since the surface of the ice rise is nowhere higher than 30 m above sea level, it is evidently grounded to a depth of 70 m or more below sea level in some places. The Marvin ice rises, with an elevation not exceeding 20 m, are also seen to be grounded below sea level. It has been shown that the Ward Hunt Ice Shelf was initiated not more than 3,000 years ago (Crary, 1960), and that sea level in relation to Ward Hunt Island has fallen 30 m in the last 7,000 years (Christie, 1967). Therefore, it is supposed that these ice rises started as part of an ice shelf forming over sea rather deeper than at present. As the ice shelf thickened, parts of it went aground to form the modern ice rises - a process assisted to some extent by isostatic rise of the land. Since Disraeli Fiord was formerly occupied by a very large glacier (Hattersley-Smith et al., 1955), it may fairly be inferred that the ice rises are grounded in shoal water caused by morainal deposition in the lea of Ward Hunt Island and the Marvin Islands. On the other hand, the radio sounding records indicate that part of the Cape Discovery ice rise is grounded above sea level. The surface elevations and ice depths at Cape Discovery are consistent with grounding at 30 m elevation in some parts, at which level on Ward Hunt Island there is a well-developed raised beach.

Summary and Conclusions

The S.P.R.I. Mark II radio echo sounding apparatus was successfully test-flown for the first time, after satisfactory arrangements had been made for installation of the radar and recording instruments in an Otter aircraft, and problems of design and installation of suitable antennas had been overcome. This success in itself justified the flying operations totalling 18

* These depths do not tally with the results of leveling by H. Serson in May 1969, which indicated a freeboard of 4.4 m for the ice shelf 3 km east of Ward Hunt Island, corresponding to an ice thickness of only 35 m.

hours in northern Ellesmere Island, particularly in view of the subsequent extensive and highly successful use of the system in Antarctica (Polar Record, 1968). At the same time, simple visual navigation, with interpolation from dead reckoning, proved adequate for plotting ice thickness profiles along flight lines up and down glaciers, and across ice caps and ice shelves.

Over the ice caps many of the flights were made near rock ridges, which was convenient for aircraft navigation, but more valuable data would have been acquired for glaciological purposes if the flights had been along lines of glacier flow. Over the glaciers, on the other hand, valuable information was obtained on subglacial profiles (particularly at glacier termini), on lengths of glaciers afloat and lengths grounded below sea level, and on occurrence of internal reflecting layers.

The most important results of the survey were as follows:

1. On the ice caps the maximum depth measured was 900 m. Very irregular topography was indicated beneath the major ice caps. Maximum ice depths ranged from 100 to 250 m for the minor ice caps.
2. On the glaciers it was found that for widths of valleys less than 2.5-3 km, interference by oblique echoes obscured the bottom echo. Maximum ice depths on all major glaciers ranged from 600 to 700 m.
3. It was possible to recognize on the radar trace a sharp break in most cases between the floating and grounded ice near termini of tidewater glaciers and at junctions between ice shelf and ice rise.
4. On the north coast of the island the fiords are shown to have subglacial extensions far to the south of the ice fronts of trunk glaciers.
5. A subglacial ridge is present beneath part of the Otto Glacier, a glacier that is known to have started to surge between 1950 and 1959.
6. Subglacial ridges occur near the snouts of glaciers on the south side of the central ice cap. These may represent moraines overridden by recent glacial advances.
7. Ice rises at Ward Hunt Island and in the mouth of Disraeli Fiord are shown to be grounded below sea level over their whole extent. Unexpectedly great ice thickness of 70 - 80 m for the ice shelf to the east of Ward Hunt Island were found.
8. Internal reflecting layers were noted in several areas, but no firm conclusions can be drawn as to their origin.

References

Bailey, J.T., Evans, S. and Robin, G. de Q. 1964. Radio echo sounding of polar ice sheets. Nature, Vol. 204, No. 4957, p. 420-21.

Christie, R.L. 1967. Reconnaissance of the surficial geology of northeastern Ellesmere Island, Arctic Archipelago. Geol. Surv. Can. Bull. 138, 50 p.

Crary, A.P. 1958. Arctic ice island and ice shelf studies, Part I. Arctic, Vol. 11, No. 1, p. 3-42.

1960, Arctic ice island and ice shelf studies, Part II. Arctic, Vol. 13, No. 1, p. 32-50.

Crowley, F.A. 1961. Density distribution for a two-layer shelf. Air Force Cambridge Research Laboratories, Geophysics Research Directorate: Proc. Third Annual Arctic Planning Session, p. 31-33.

Evans, S. and Robin, G. de Q. 1966. Glacier depth-sounding from the air. Nature, Vol. 210, No. 5039, p. 883-85.

Evans, S. and Smith, B.M.E. 1969. A radio echo apparatus for sounding polar ice sheets. J. Scient. Instr. Ser. 2, Vol. 2, p. 131-36.

Faig, W. 1966. Photogrammetry applied to Arctic glacier surveys. Defence Research Board: Report D Phys R (G) Hazen 27, 56 p.

Hattersley-Smith, G. 1963a. Climatic inferences from firn studies in northern Ellesmere Island. Geogr. Annaler, Vol. 45, No. 2-3, p. 139-51.

1963b. The Ward Hunt Ice Shelf: recent changes of the ice front. J. Glaciol., Vol. 4, No. 34, p. 415-24.

1964. Rapid advance of glacier in northern Ellesmere Island. Nature, Vol. 20, No. 4915, p. 176.

1967. Note on ice shelves off the north coast of Ellesmere Island. Arctic Circular, Vol. 17, No. 1 (1965-66), p. 13-14.

1969. Glacial features of Tanquary Fiord and adjoining areas of northern Ellesmere Island, N.W.T. J. Glaciol., Vol. 8, No. 52 (in press).

Hattersley-Smith, G. and Serson, H. 1966. Reconnaissance oceanography over the ice of the Nansen Sound fiord system. Defence Research Board: Report D Phys R (G) Hazen 28, 18 p.

Hattersley-Smith, G., Crary, A.P. and Christie, R.L. 1955. Northern Ellesmere Island, 1953 and 1954. Arctic, Vol. 8, No. 1, p. 3-36.

Konecny, G. 1966. Applications of photogrammetry to surveys of glaciers in Canada and Alaska. Can. J. Earth Sci., Vol. 3, No. 6, p. 783-98.

Lyons, J.B. and Leavitt, F.G. 1961. Structural-stratigraphic studies on the Ward Hunt Shelf. Air Force Cambridge Research Laboratories, Geophysics Research Directorate: Final Report on Contract AF (604)-6188, 36 p.

Lyons J.B. and Ragle, R.H. 1962. Thermal history and growth of the Ward Hunt Shelf. Commission of Snow and Ice, I.A.S.H. Pub. No. 58, p.88-97.

(Polar Record). 1968. Radio echo exploration of the Antarctic ice sheet,1967. Polar Record, Vol. 14, No. 89, p. 211-13.

Ragle, R.H., Blair, R.G. and Persson, L.E. 1964. Ice core studies of Ward Hunt Ice Shelf, 1960. J. Glaciol. Vol. 5, No. 37, p. 39-59.

Robin, G. de Q. 1969. Initiation of Glacier Surges. Can. J. Earth Sci., (in press).

Robin, G. de Q., Evans, S. and Bailey, J.T. 1969. Interpretation of radio echo soundings in polar ice sheets. Phil. Trans. Roy. Soc. London (in press).

Weber, J.R. 1961. Comparison of gravity and seismic depth determinations on the Gilman Glacier and adjoining ice cap in northern Ellesmere Island in Raasch, G.O. (Ed). Geology of the Arctic (Vol. 2). University of Toronto Press: p. 981-90.

Weber, J.R., Sandstrom, H. and Arnold, K.C. 1961. Geophysical surveys on Gilman Glacier, northern Ellesmere Island. Commission of Snow and Ice, I.A.S.H. Pub. No. 54, p. 500-11.

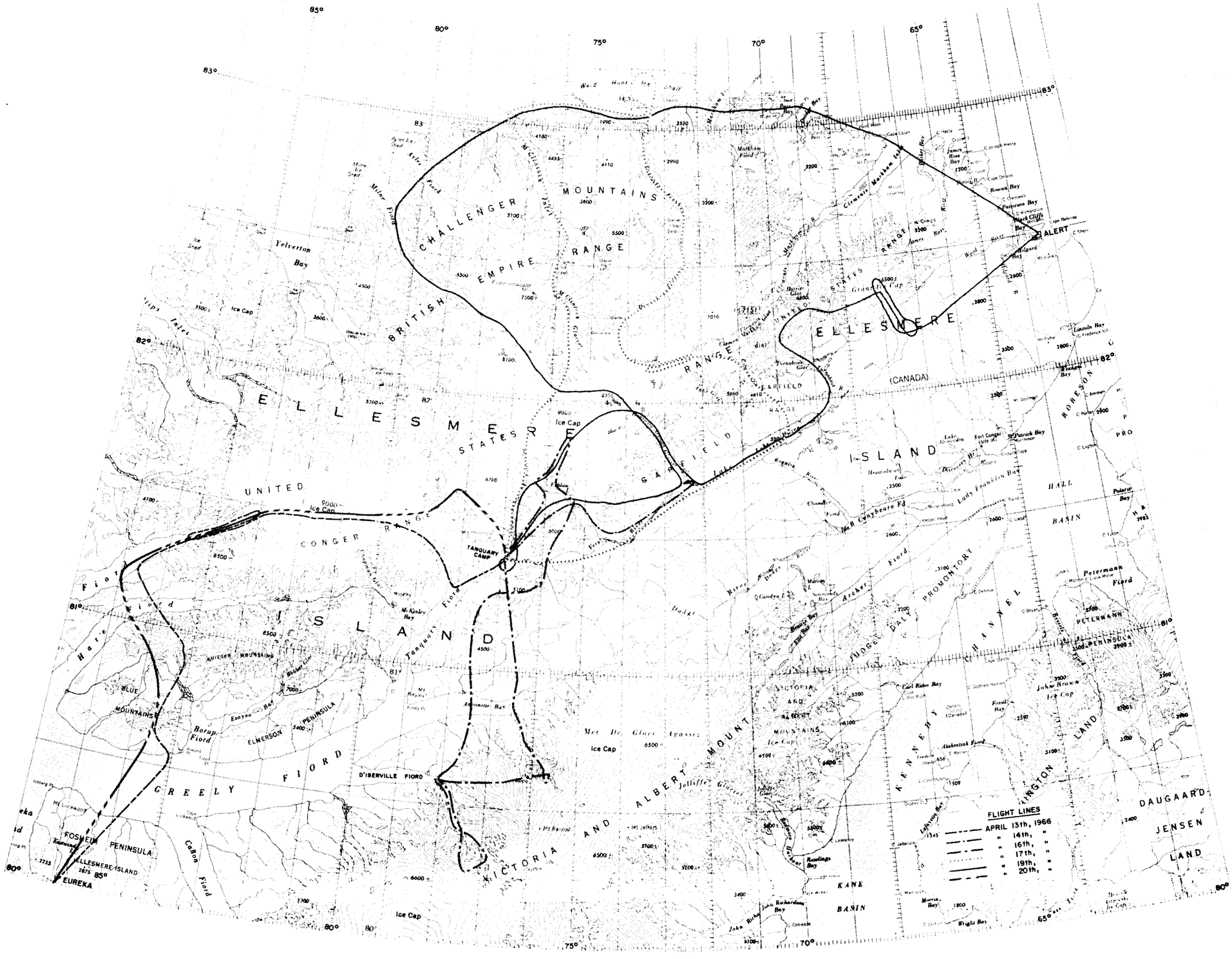

CHALLENGER MOUNTAINS
BRITISH EMPIRE RANGE
ELLESMERE ISLAND
UNITED STATES RANGE
GARFIELD RANGE
CONGER RANGE
TANQUARY CAMP
ALERT
(CANADA)
GREELY FIORD
D'IBERVILLE FIORD
VICTORIA AND ALBERT MOUNTAINS
JUDGE DALY PROMONTORY
KENNEDY CHANNEL
HALL BASIN
KANE BASIN
DAUGAARD-JENSEN LAND
FOSHEIM PENINSULA
EUREKA
FLIGHT LINES
APRIL 13th, 1966
" 14th, "
" 16th, "
" 17th, "
" 19th, "
" 20th, "

Fig.1

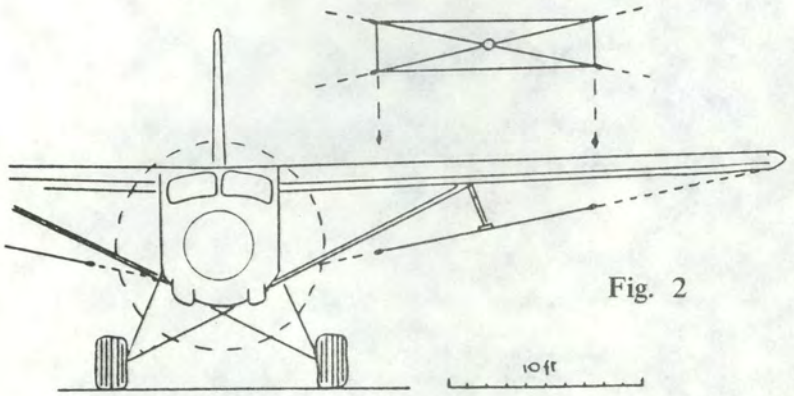

Fig. 2

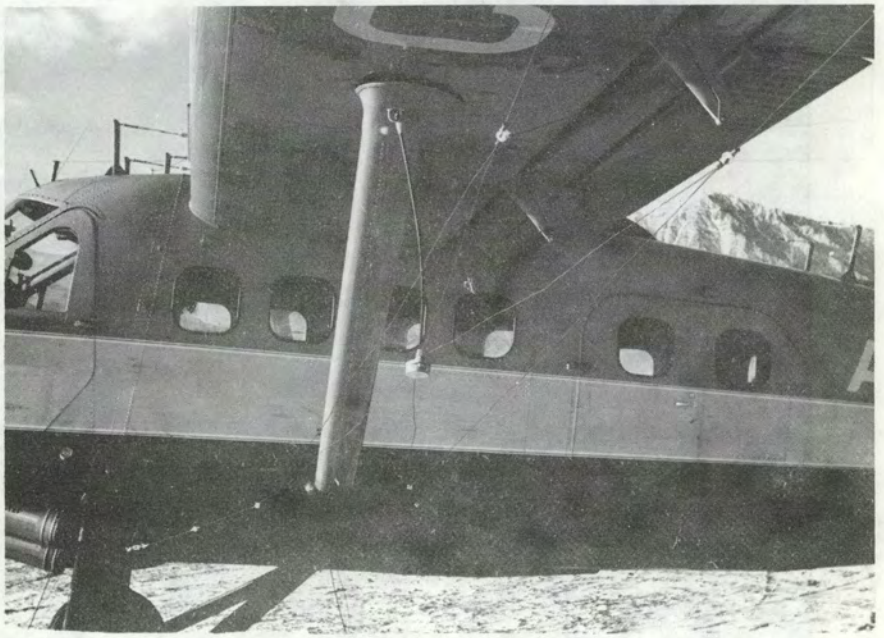

Fig. 3

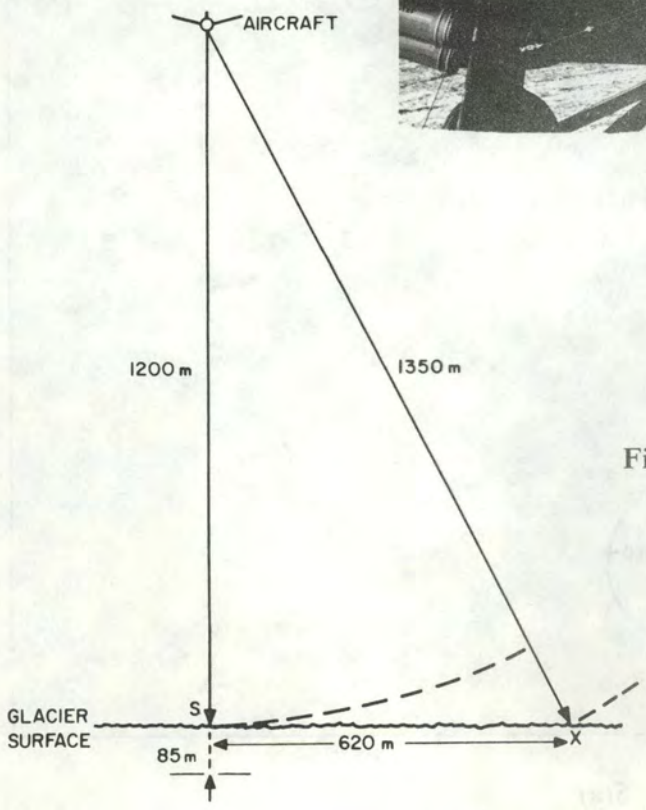

Fig. 4

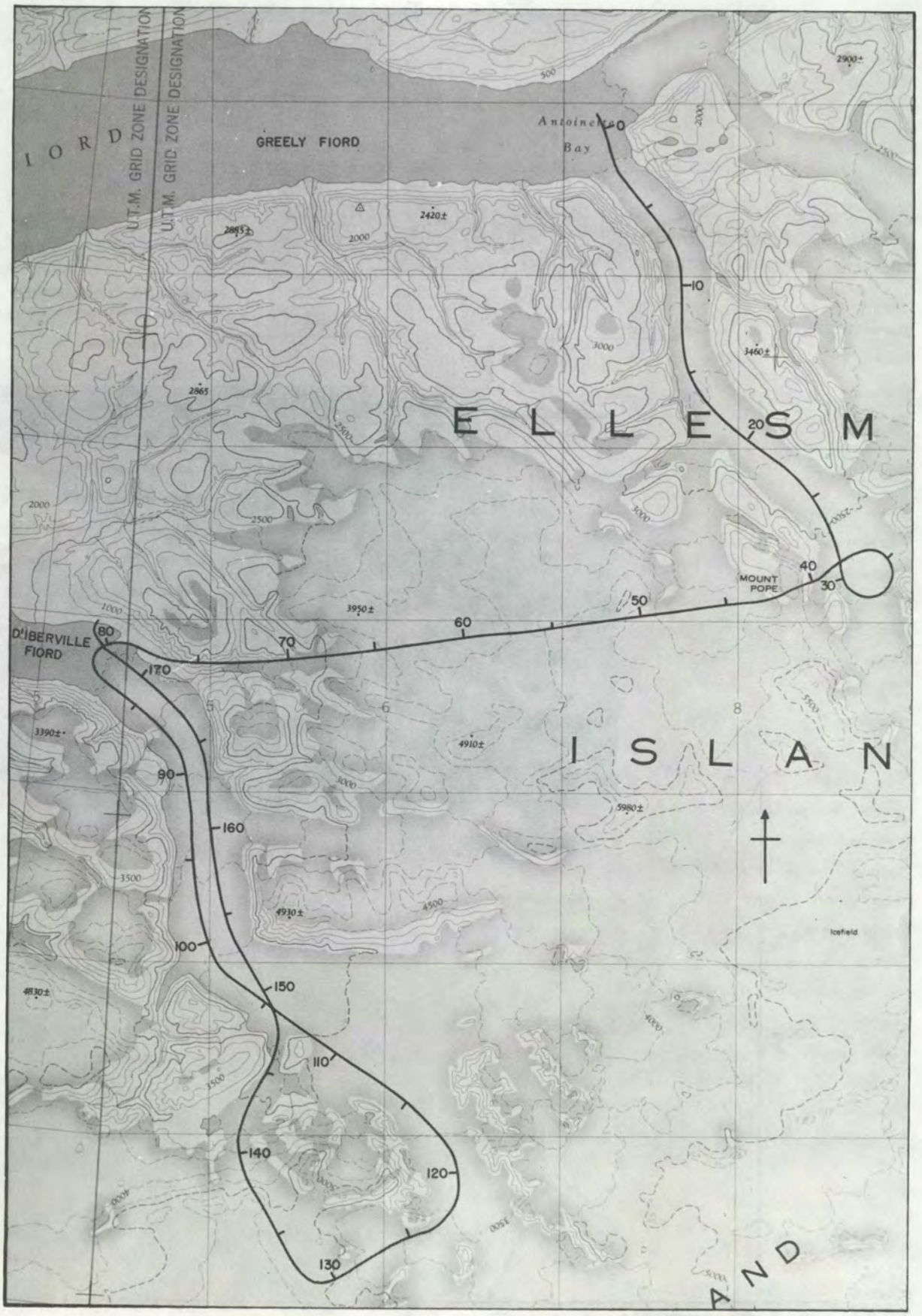

U.T.M. GRID ZONE DESIGNATION
U.T.M. GRID ZONE DESIGNATION
GREELY FIORD
Antoinette Bay
ELLESM
ISLAN
AND
MOUNT POPE
D'IBERVILLE FIORD
Icefield
0
10
20
30
40
50
60
70
80
90
100
110
120
130
140
150
160
170
2900±
2420±
2865
3460±
3950±
3390±
4910±
5980±
4930±
4830±

Fig. 5(a)

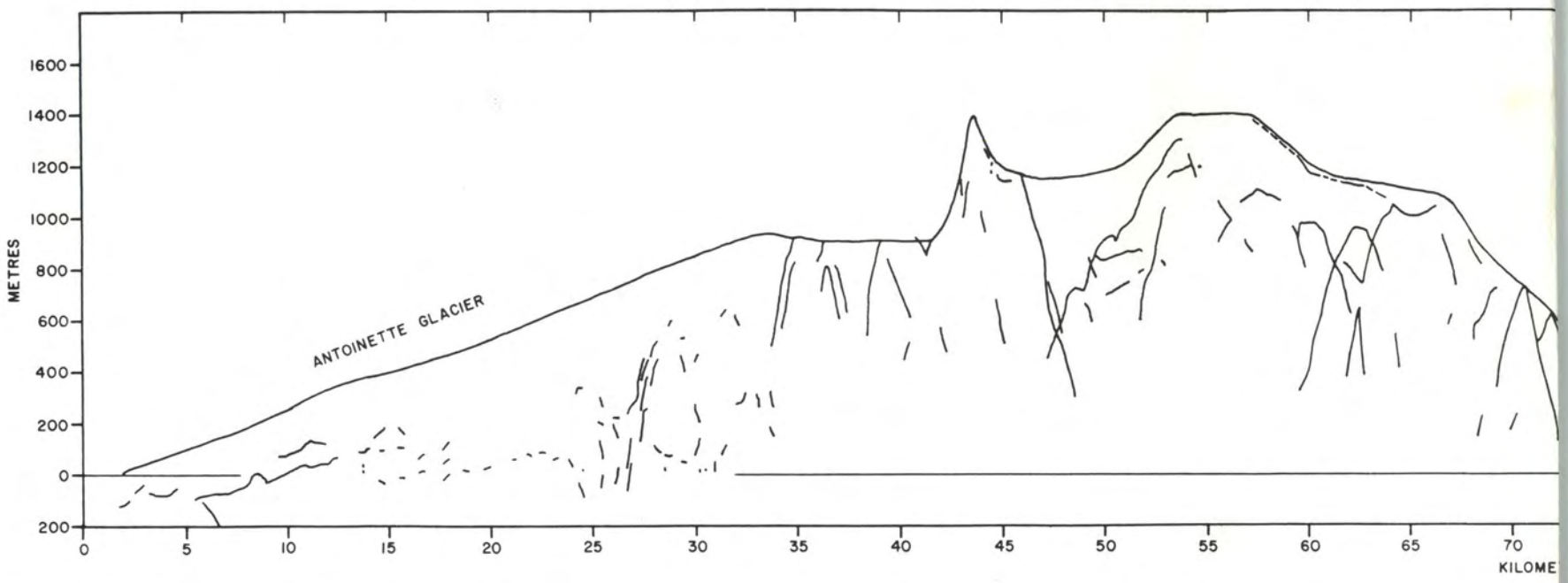
METRES
1600
1400
1200
1000
800
600
400
200
0
200
ANTOINETTE GLACIER
0
5
10
15
20
25
30
35
40
45
50
55
60
65
70
KILOME

Fig.

0
200 M INTERVALS

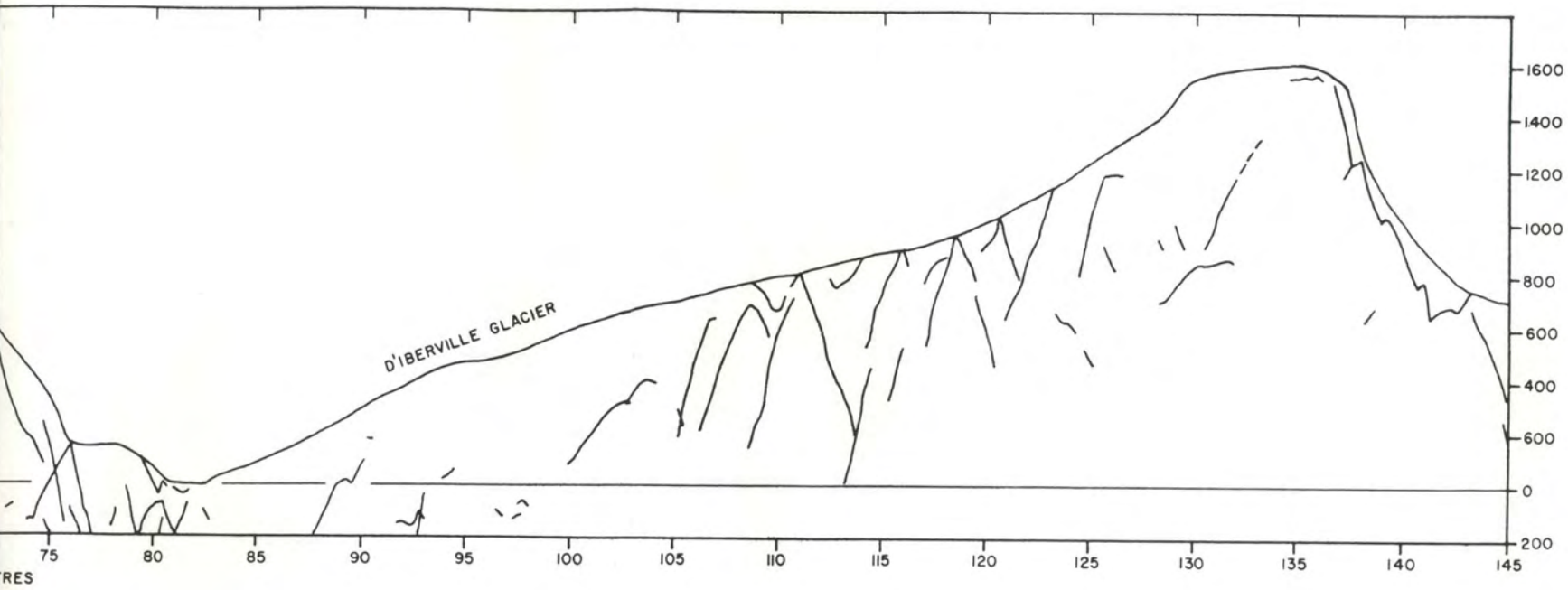
D'IBERVILLE GLACIER
1600
1400
1200
1000
800
600
400
600
0
200
75
80
85
90
95
100
105
110
115
120
125
130
135
140
145
TRES

5(b)

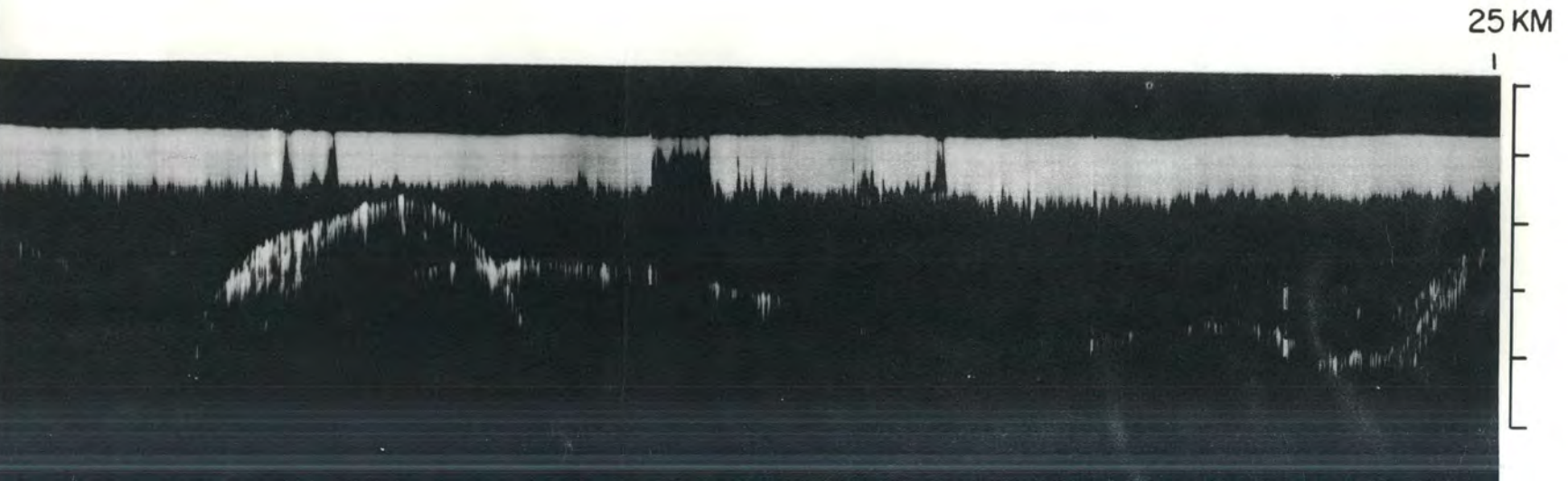
25 KM

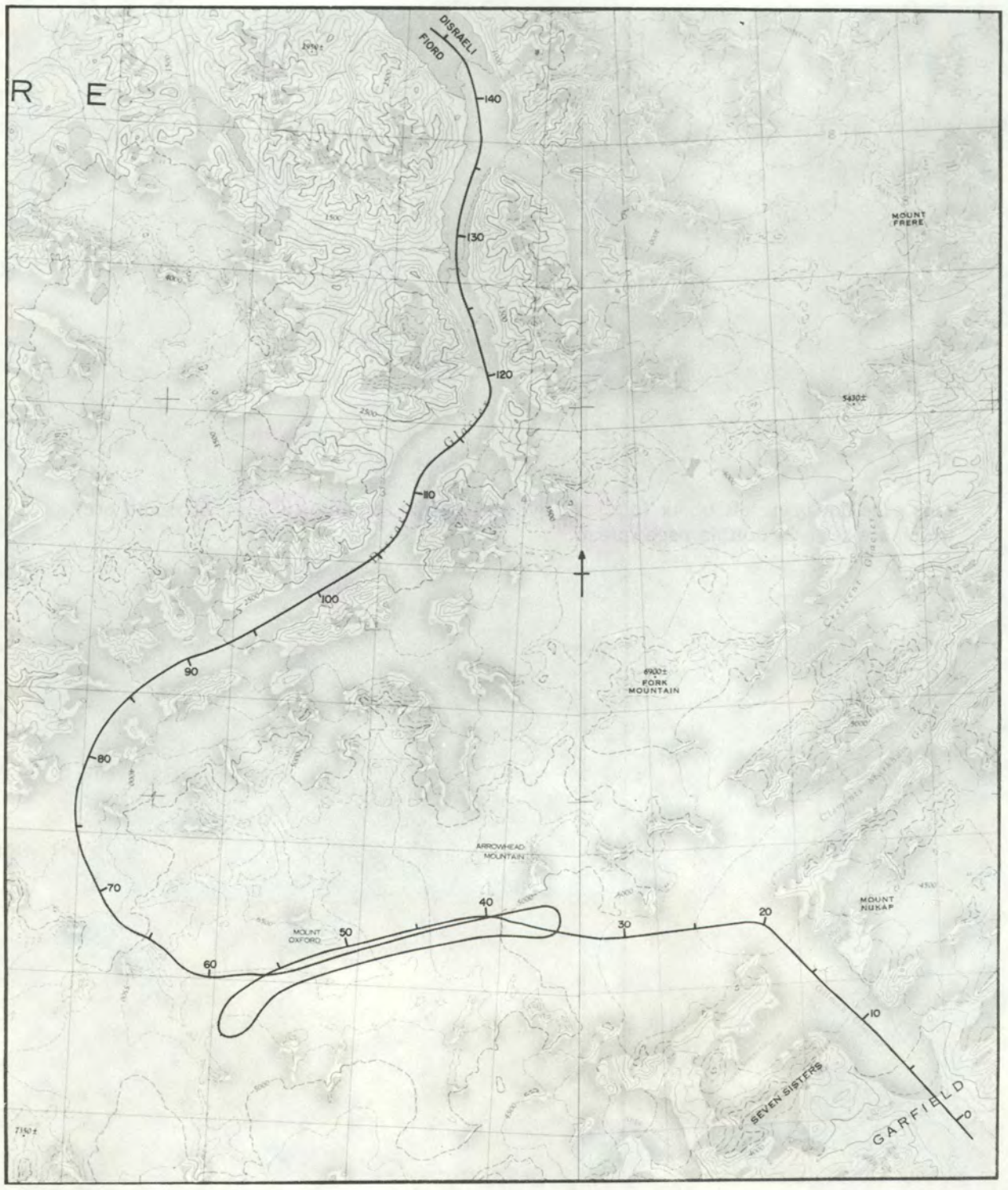
DISRAELI FIORD
R E
MOUNT FRERE
5430±
6930±
FORK MOUNTAIN
ARROWHEAD MOUNTAIN
MOUNT OXFORD
MOUNT NUKAP
SEVEN SISTERS
GARFIELD
7150±
140
130
120
110
100
90
80
70
60
50
40
30
20
10
0

Fig. 6(a)

This page has been left blank to allow Fig. 6(a) to appear opposite Figs. 6(b) and 6(c) which are set as a double page spread.

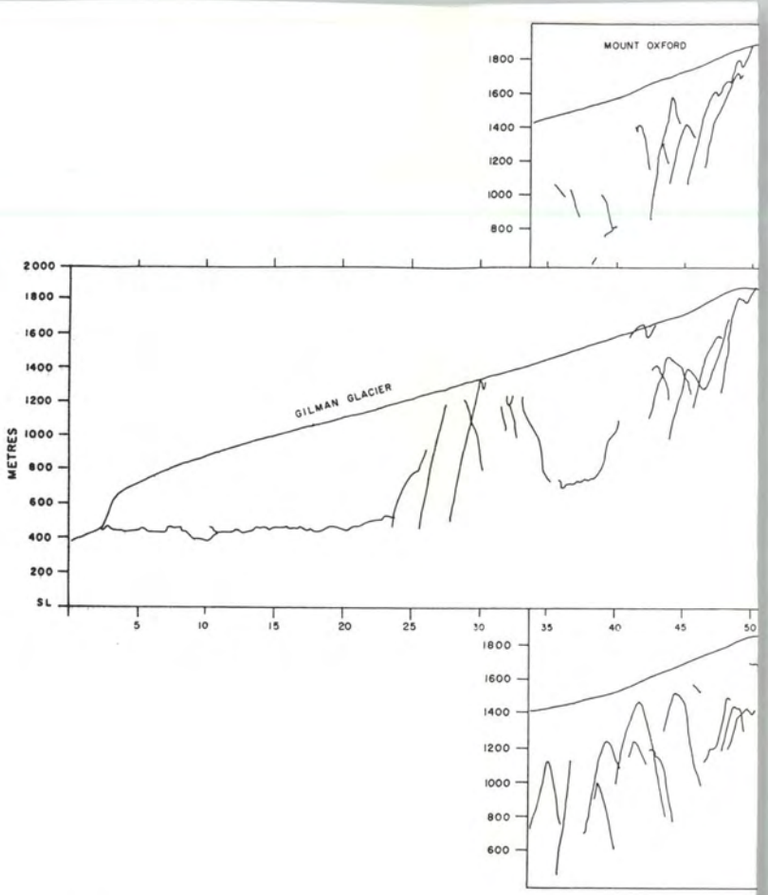
MOUNT OXFORD
GILMAN GLACIER
METRES
SL

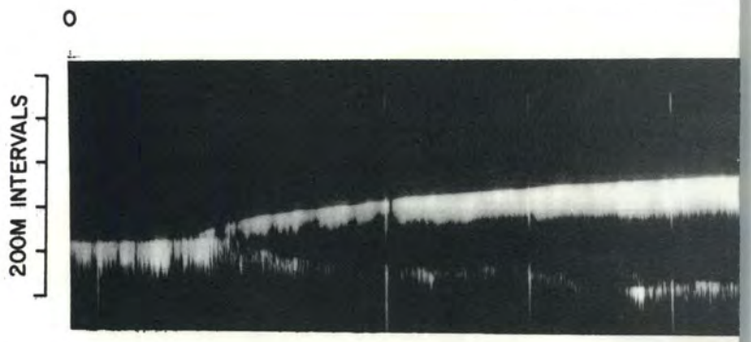
0
200M INTERVALS

Fig.6(c)
cont.

90KM
200 M INTERVALS

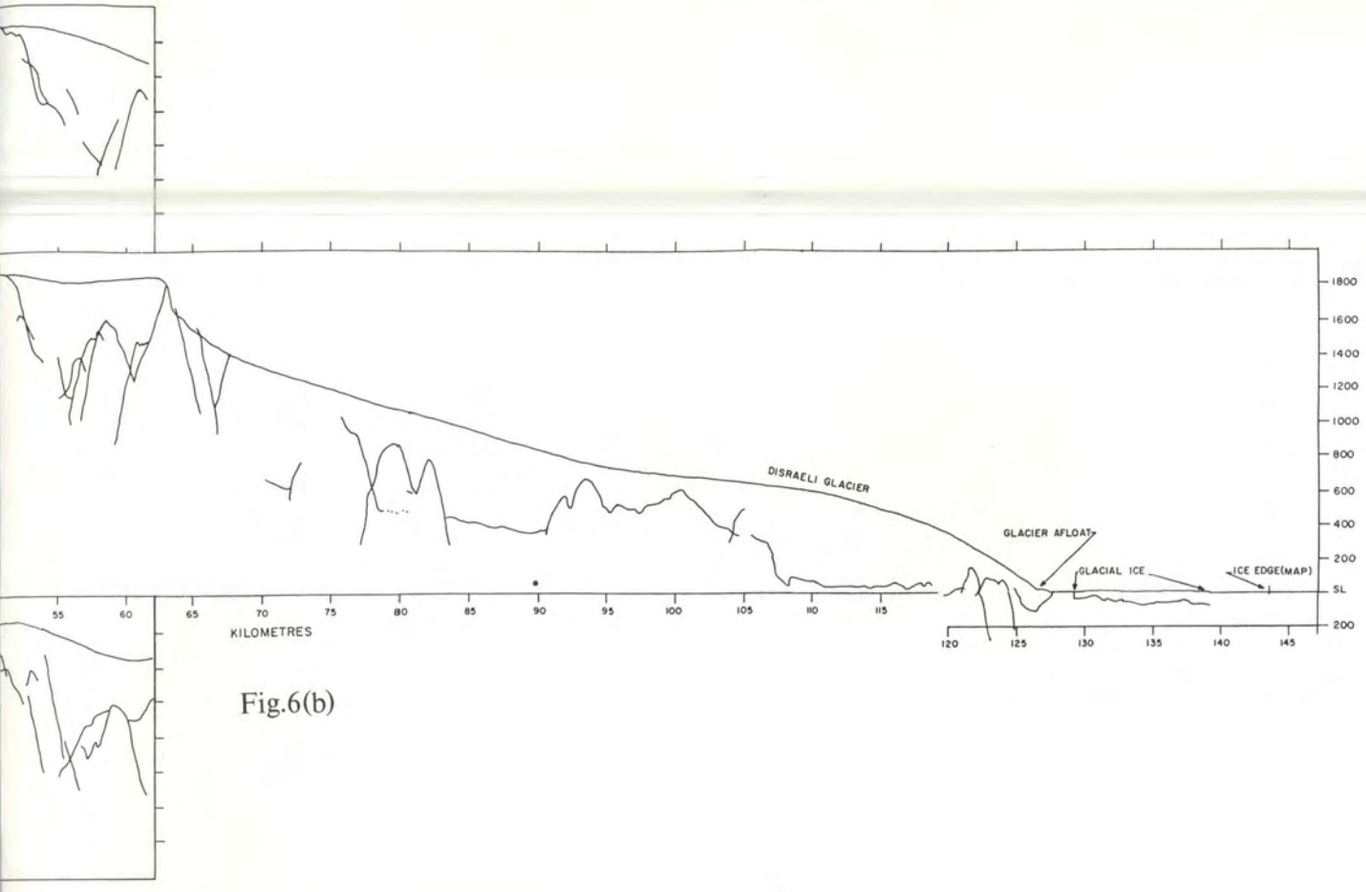

Fig.6(b)

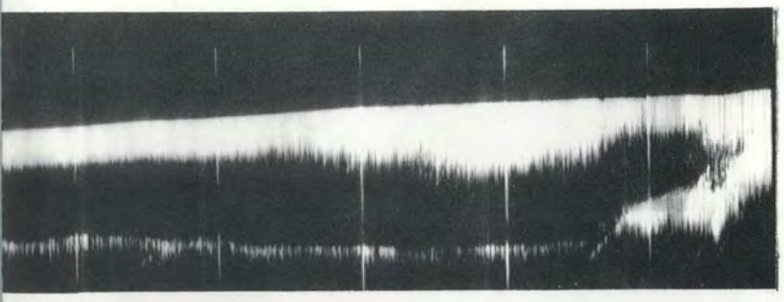

Fig.6(c)

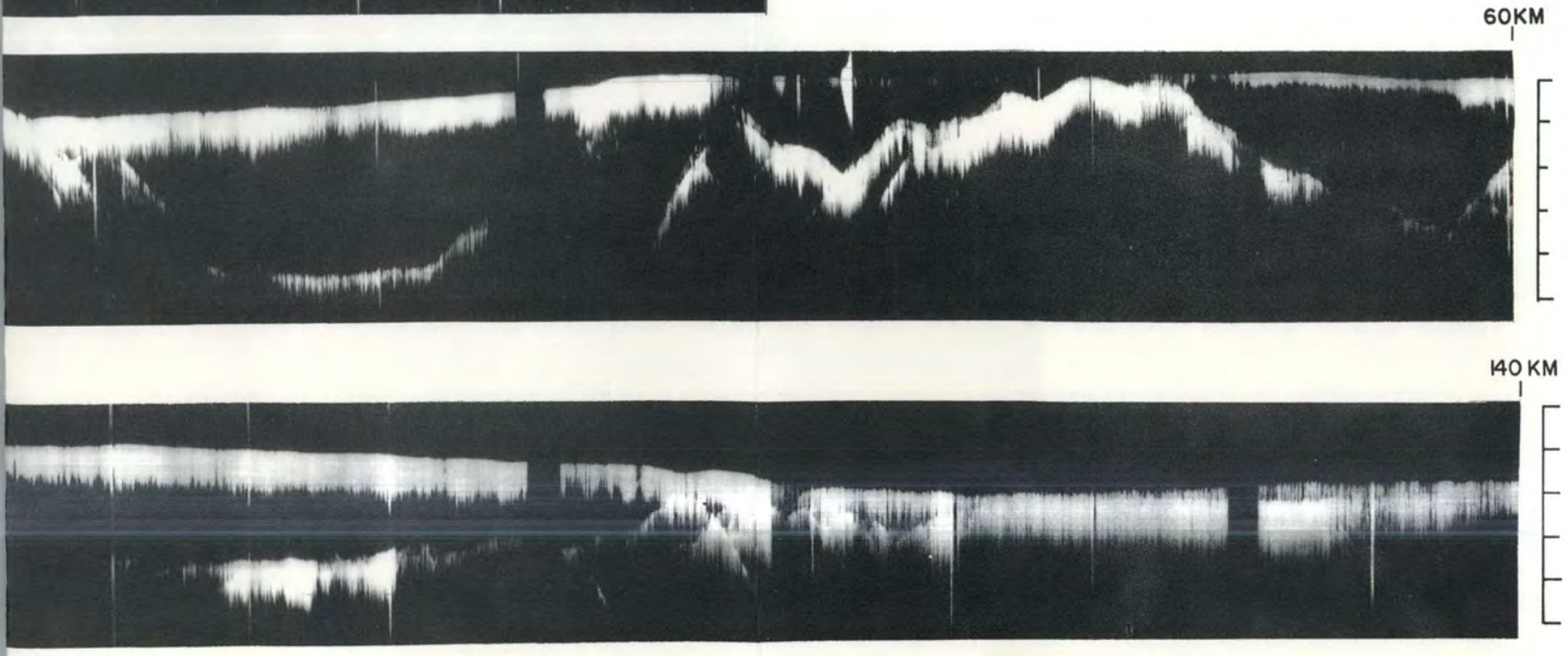

Fig.6(d)

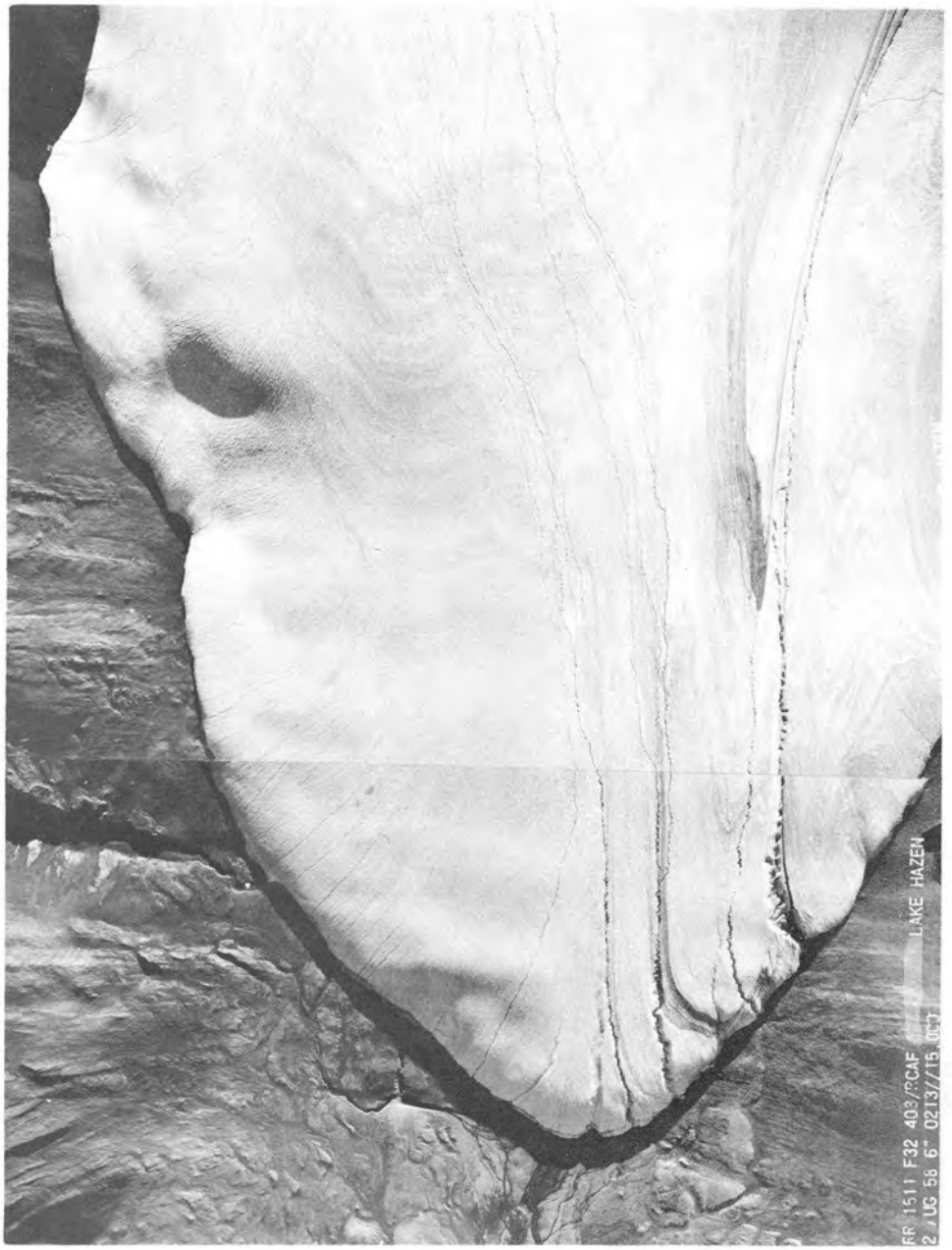

Fig. 7

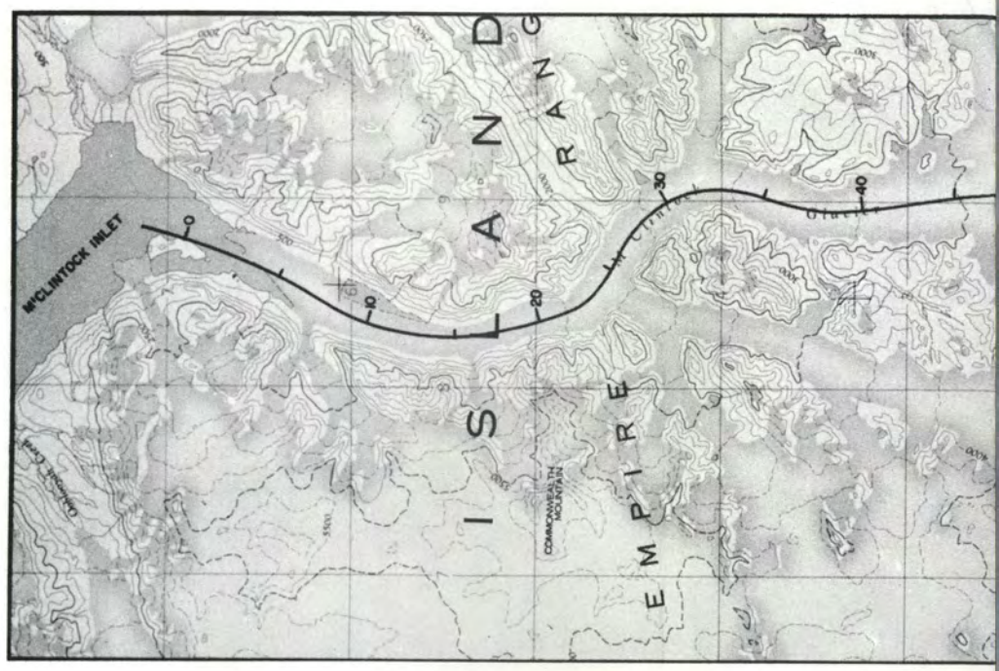
M'CLINTOCK INLET
0
10
20
30
40
ISLAND
RANGE
EMPIRE
COMMONWEALTH MOUNTAIN

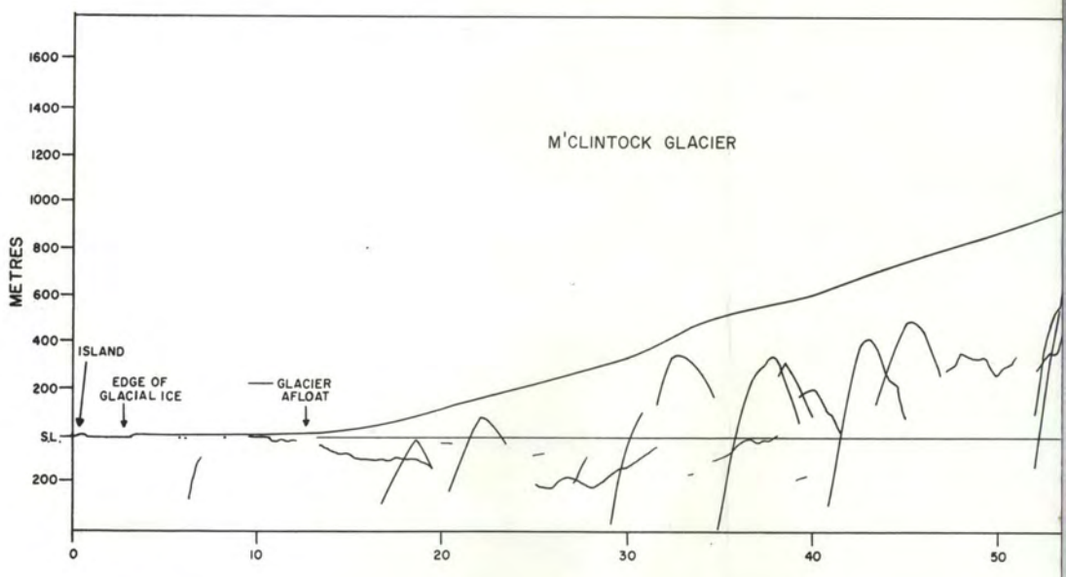
M'CLINTOCK GLACIER
METRES
1600
1400
1200
1000
800
600
400
200
S.L.
200
ISLAND
EDGE OF GLACIAL ICE
GLACIER AFLOAT
0
10
20
30
40
50

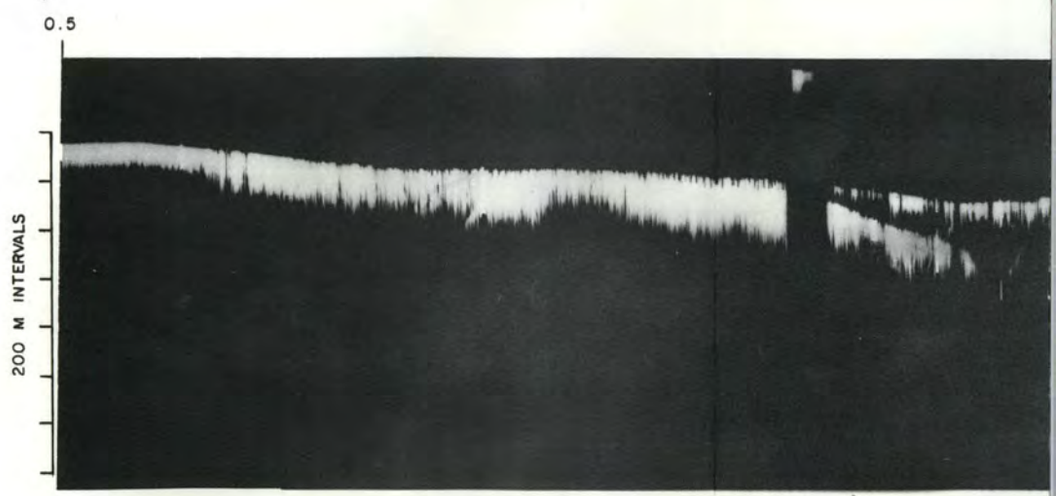
0.5
200 M INTERVALS

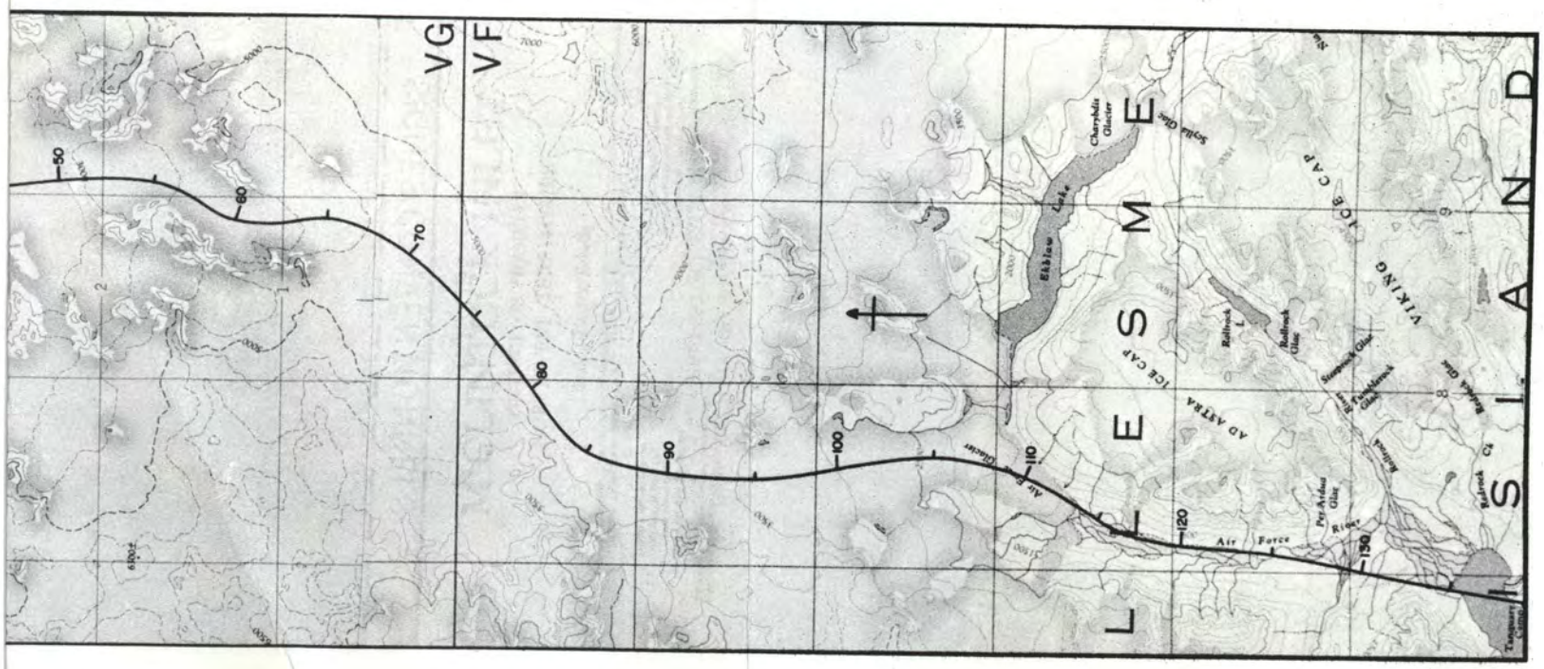

Fig. 8(a)

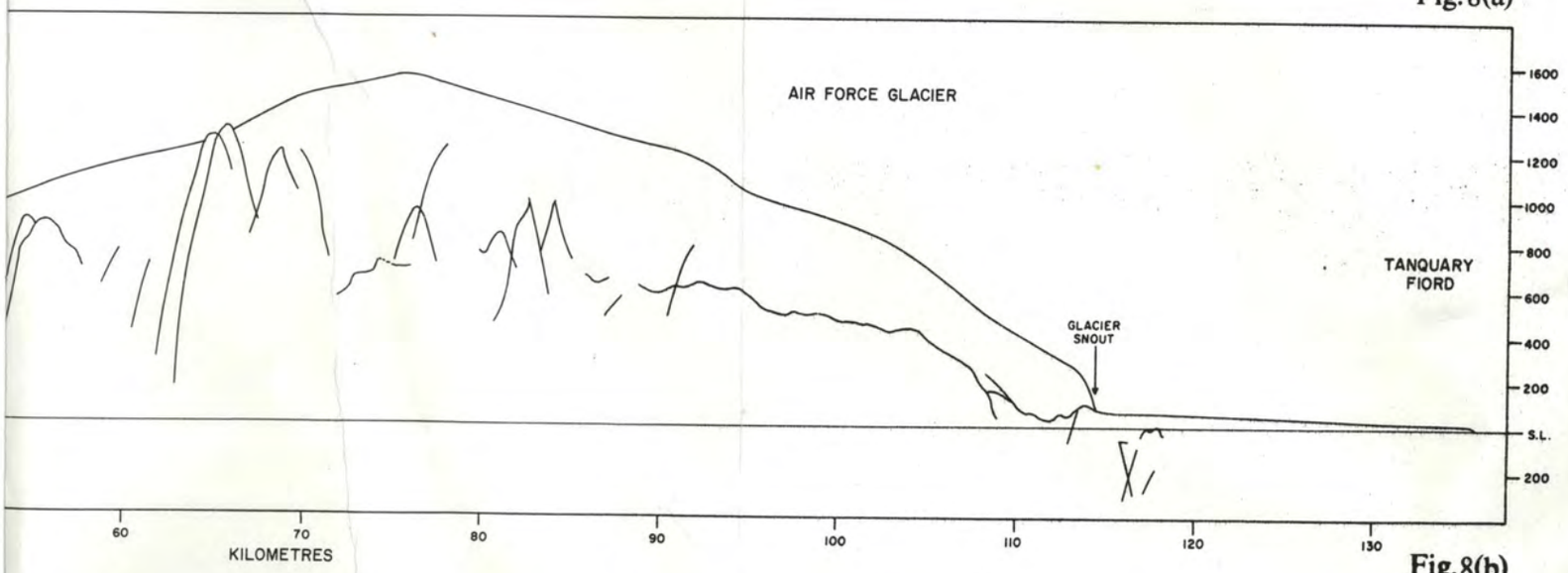

Fig. 8(b)

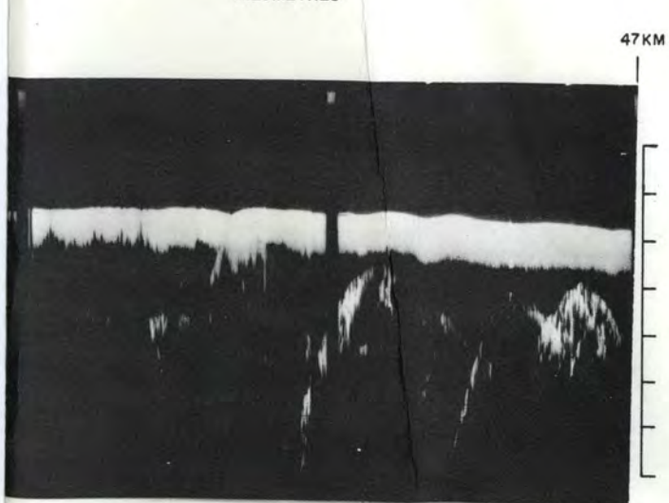

Fig. 8(c)

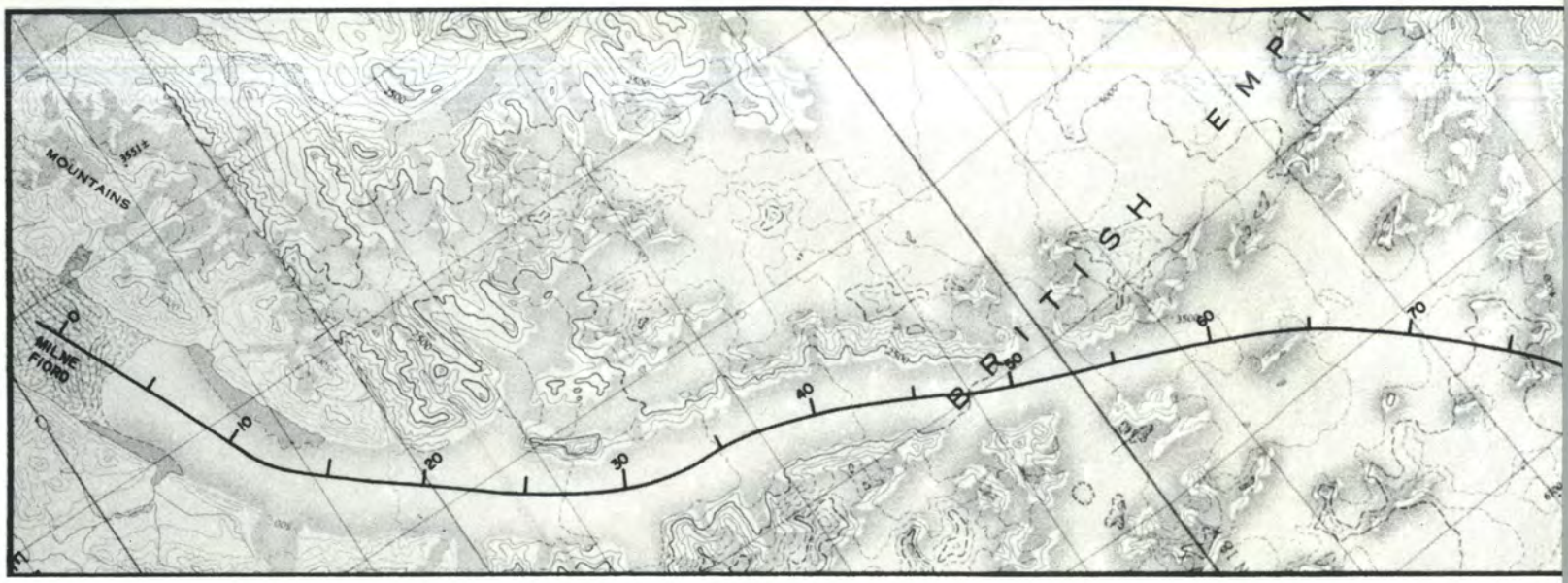
MOUNTAINS
MILNE FIORD
10
20
30
40
50
60
70
B R I T I S H E M P

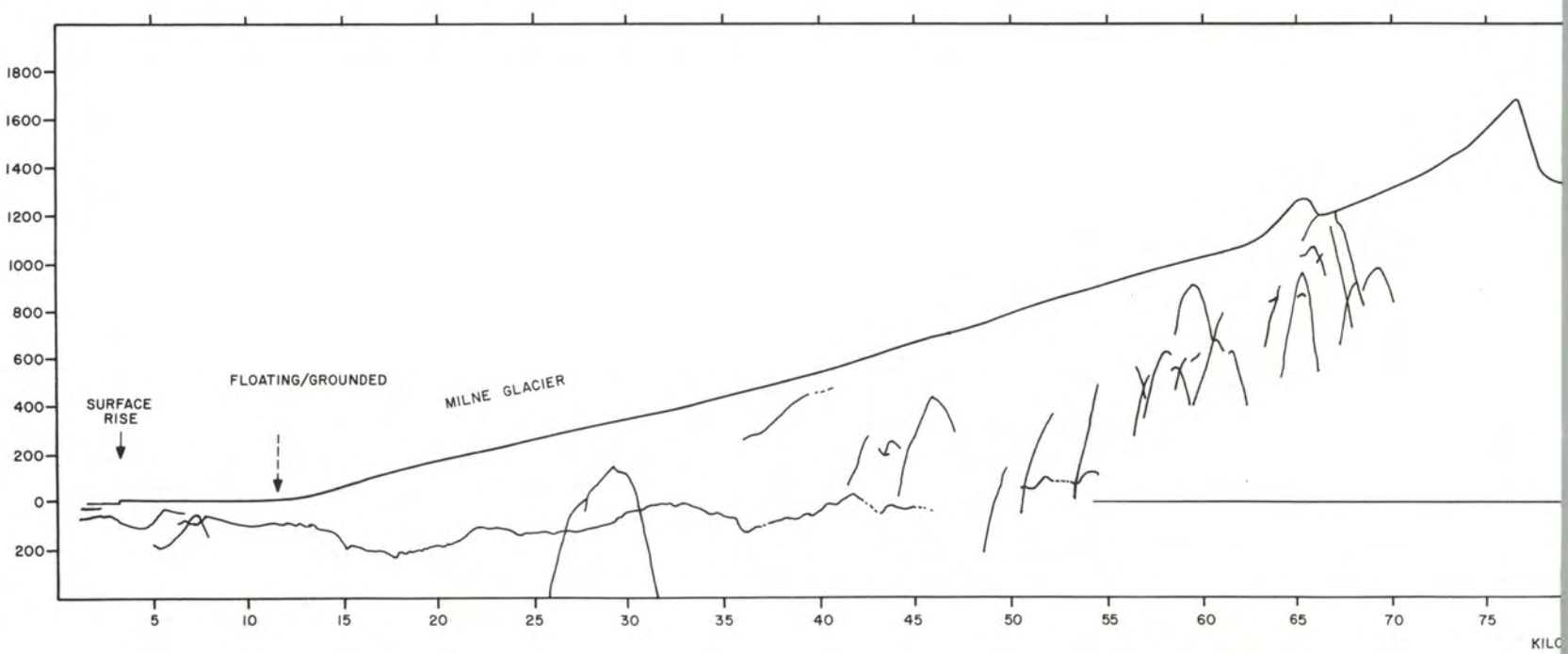
1800
1600
1400
1200
1000
800
600
400
200
0
200
SURFACE RISE
FLOATING/GROUNDED
MILNE GLACIER
5
10
15
20
25
30
35
40
45
50
55
60
65
70
75
KILO

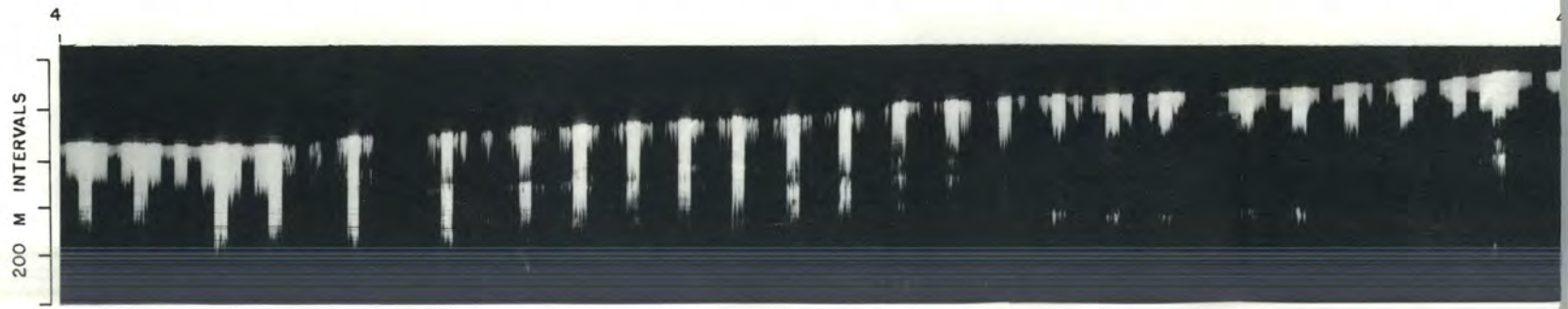
4
200 M INTERVALS

Fig.9(c)

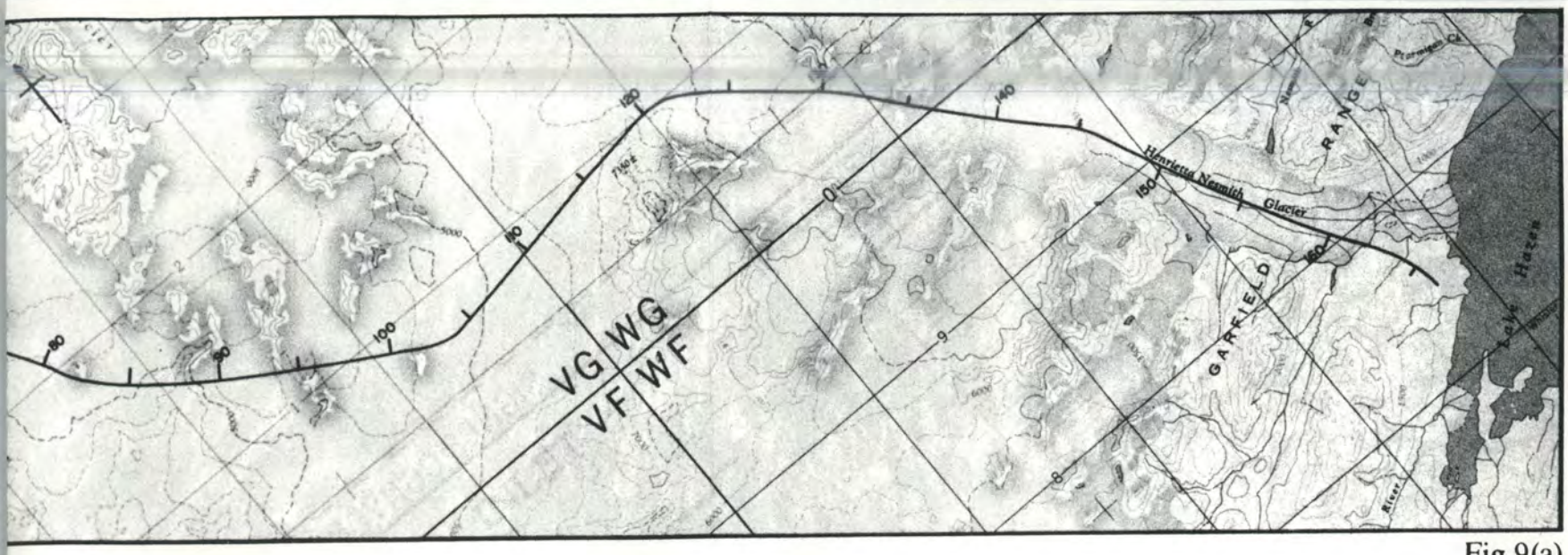

Fig.9(a)

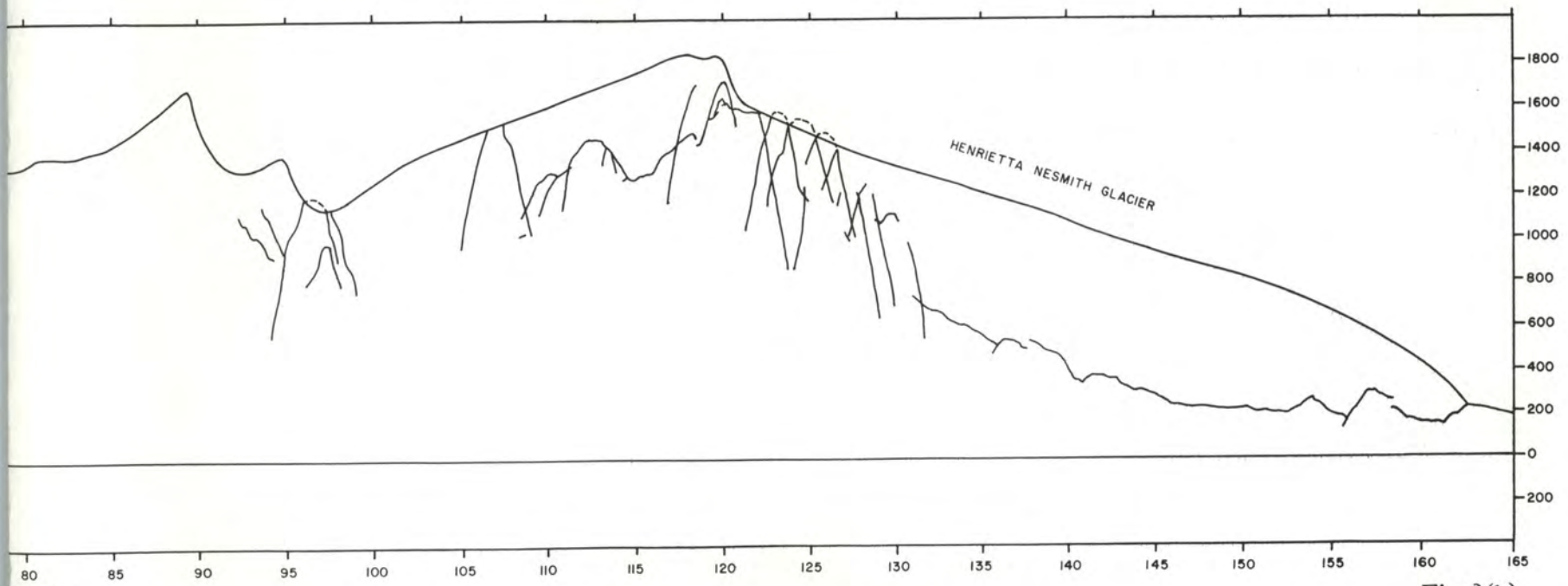

Fig.9(b)

Fig.9(d)

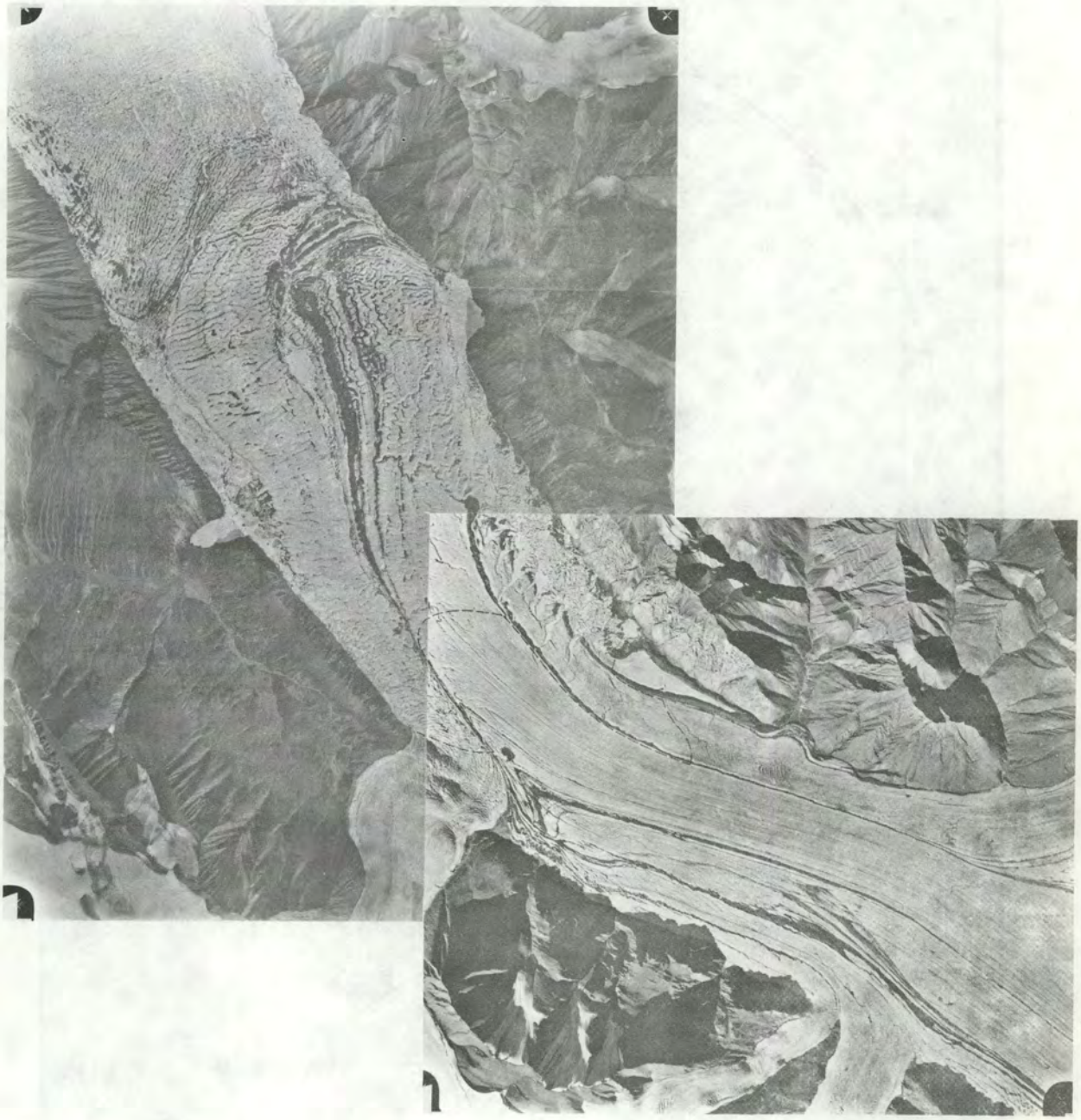

Fig. 10

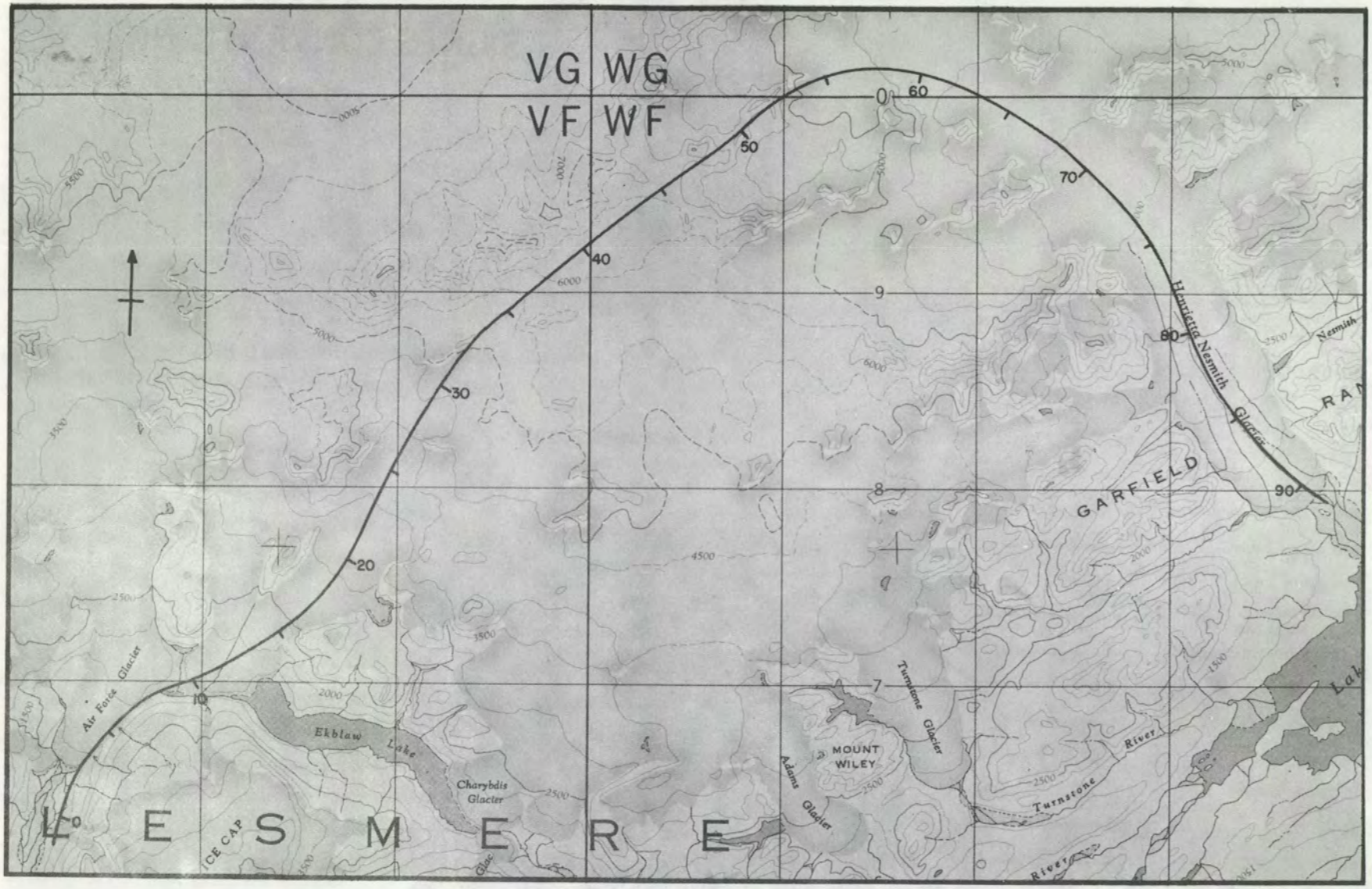
VG WG
VF WF
0
10
20
30
40
50
60
70
80
90
9
8
7
Henrietta Nesmith Glacier
GARFIELD
Nesmith
Air Force Glacier
Ekblaw Lake
Charybdis Glacier
MOUNT WILEY
Adams Glacier
Turnstone Glacier
Turnstone River
River
L E S M E R E
ICE CAP

Fig. 11(a)

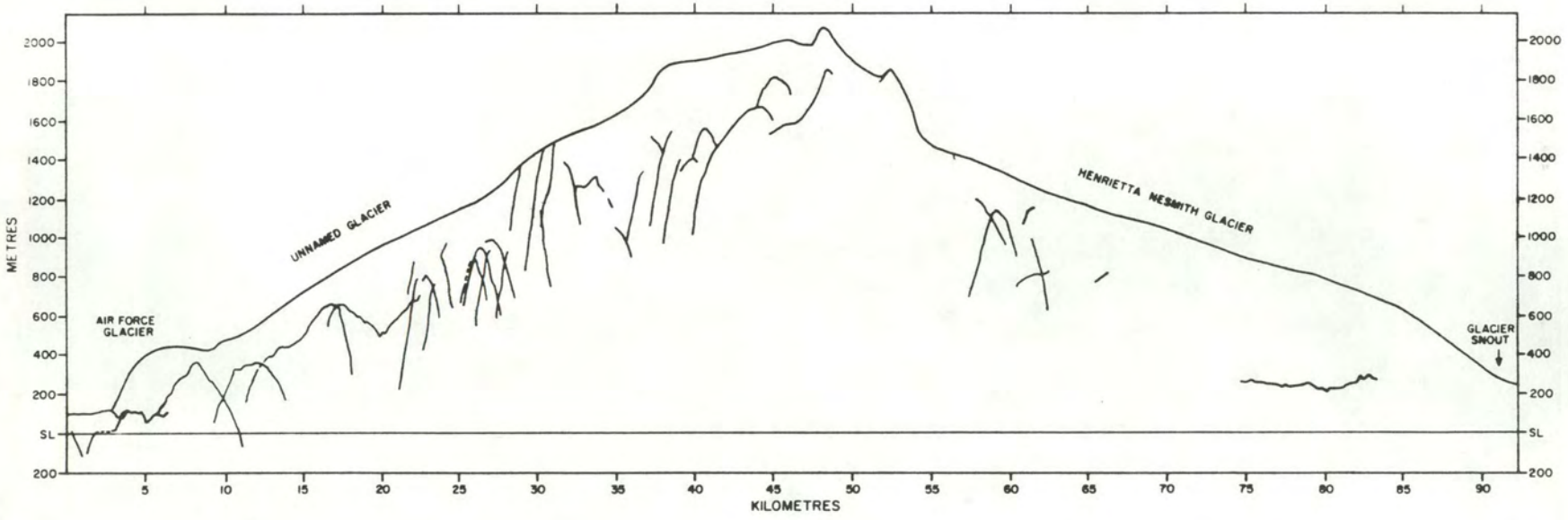
METRES
2000
1800
1600
1400
1200
1000
800
600
400
200
SL
200
UNNAMED GLACIER
AIR FORCE GLACIER
HENRIETTA NESMITH GLACIER
GLACIER SNOUT
5
10
15
20
25
30
35
40
45
50
55
60
65
70
75
80
85
90
KILOMETRES

Fig. 11(b)

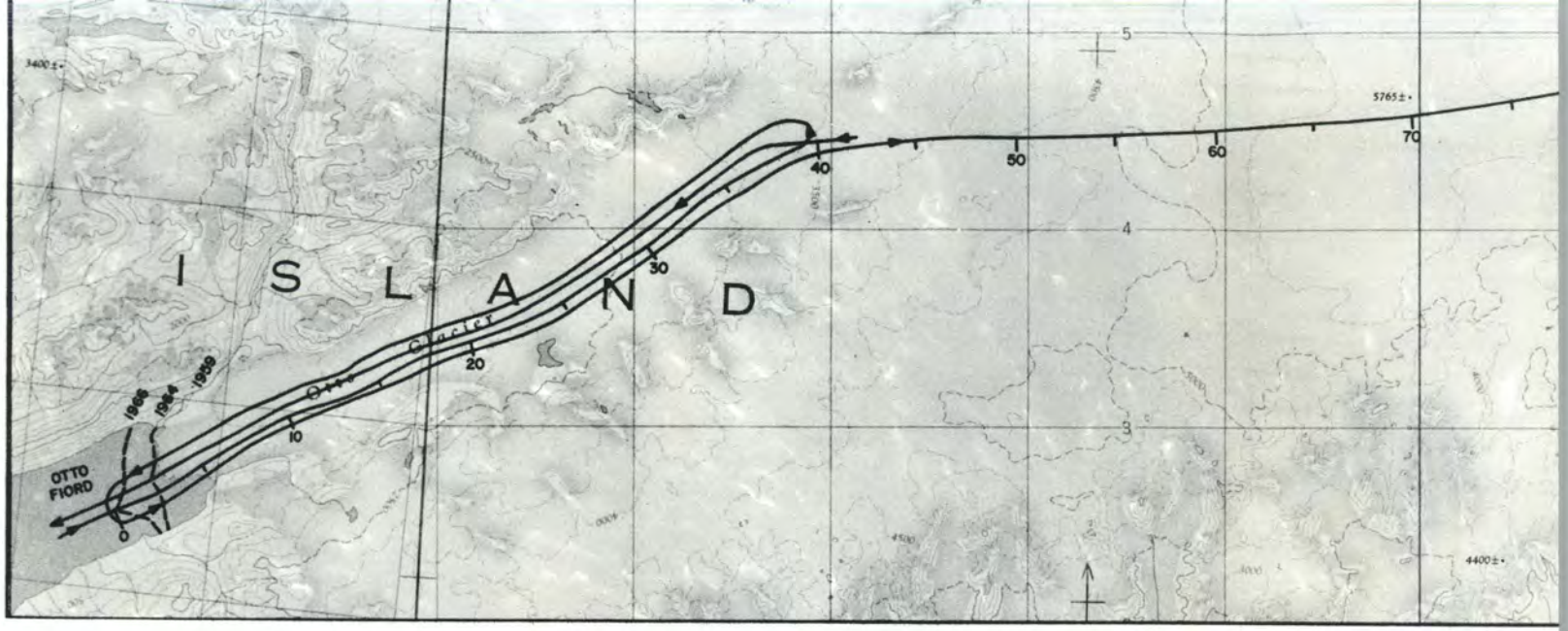
I S L A N D
Otto Glacier
OTTO FIORD
1966
1964
1959
0
10
20
30
40
50
60
70
5765±
4400±

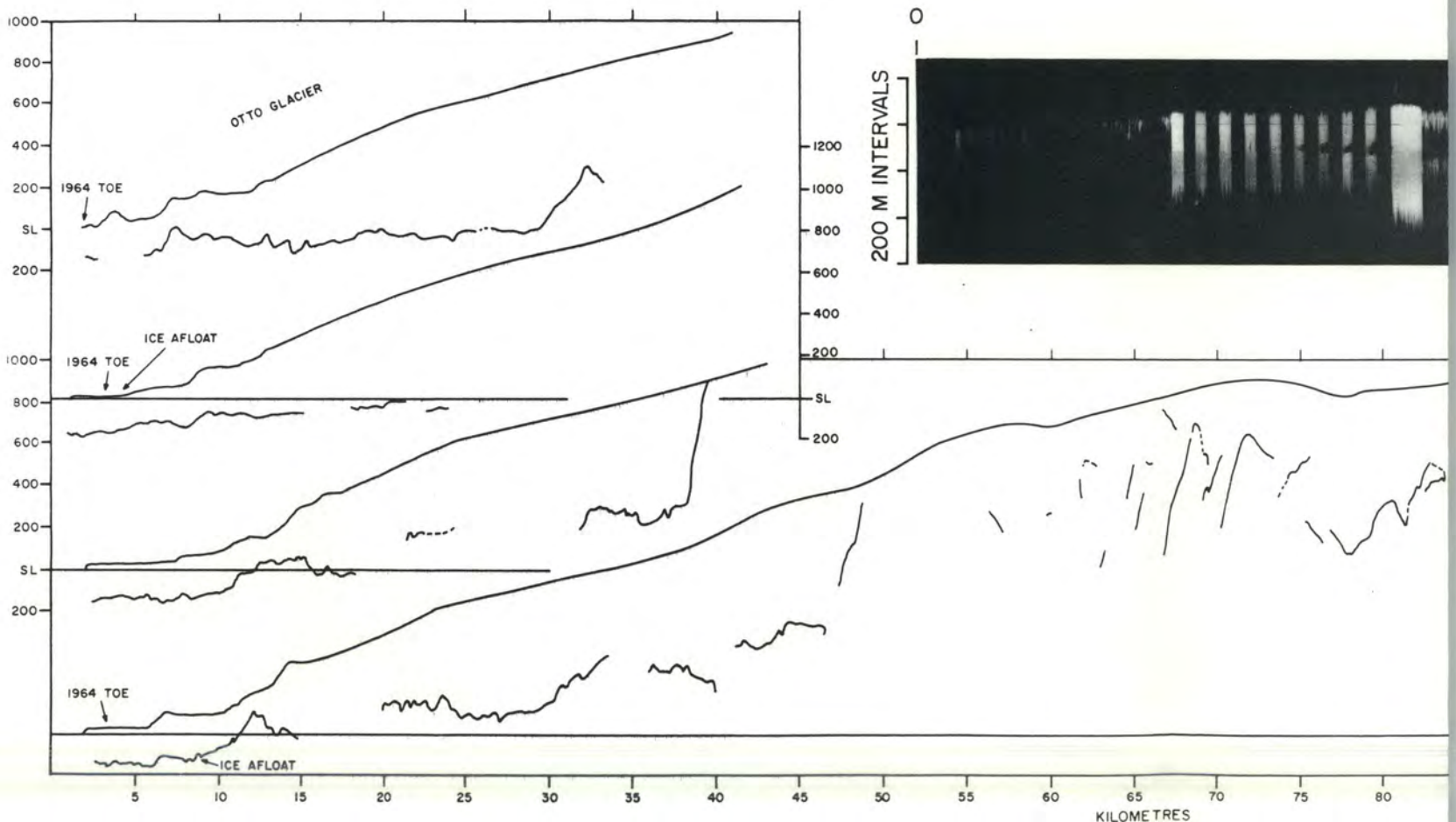
OTTO GLACIER
1964 TOE
ICE AFLOAT
SL
200 M INTERVALS
KILOMETRES
5
10
15
20
25
30
35
40
45
50
55
60
65
70
75
80

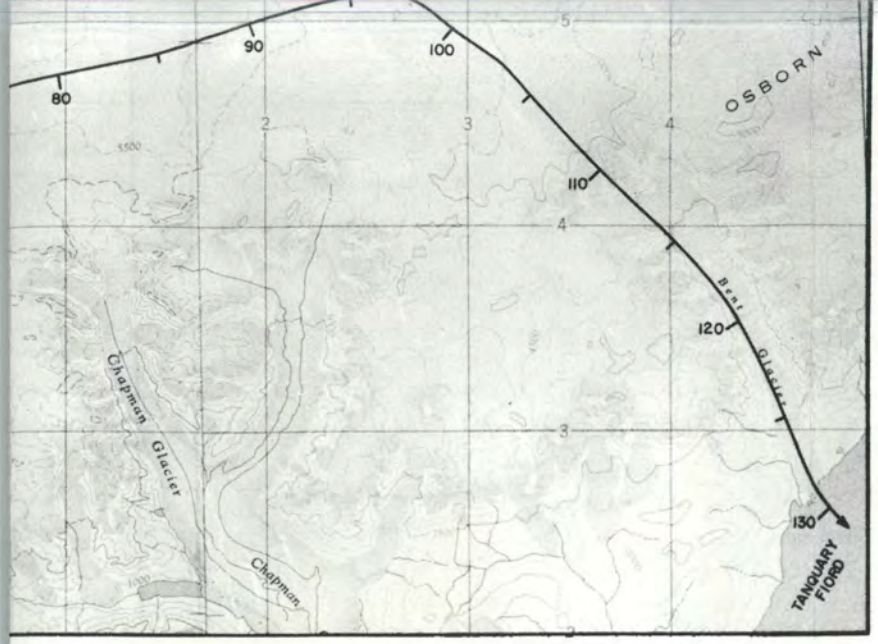

Fig. 12(a)

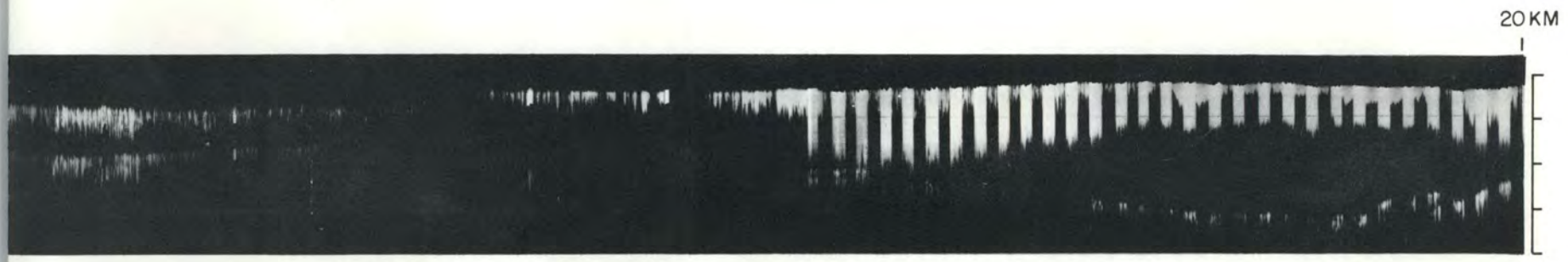

Fig. 12(c)

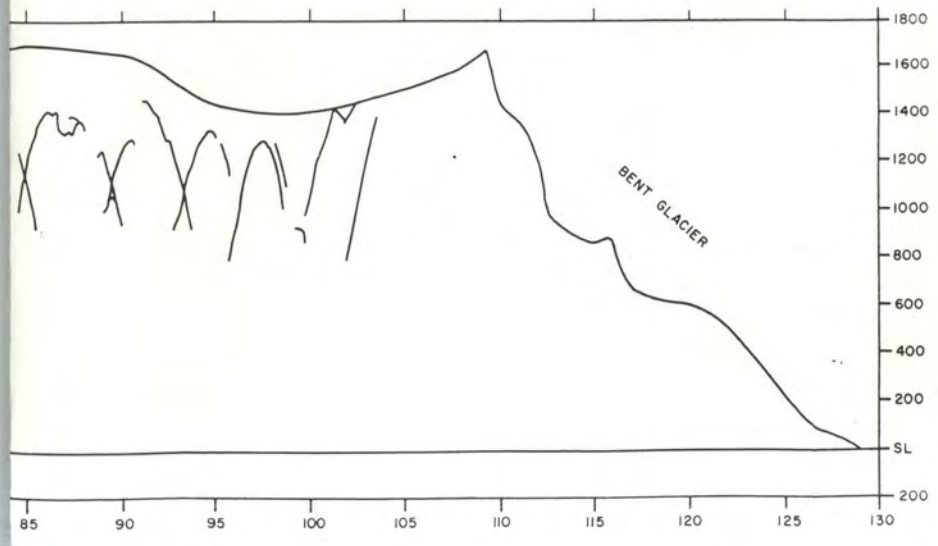

Fig. 12(b)

Fig. 13

Fig. 14

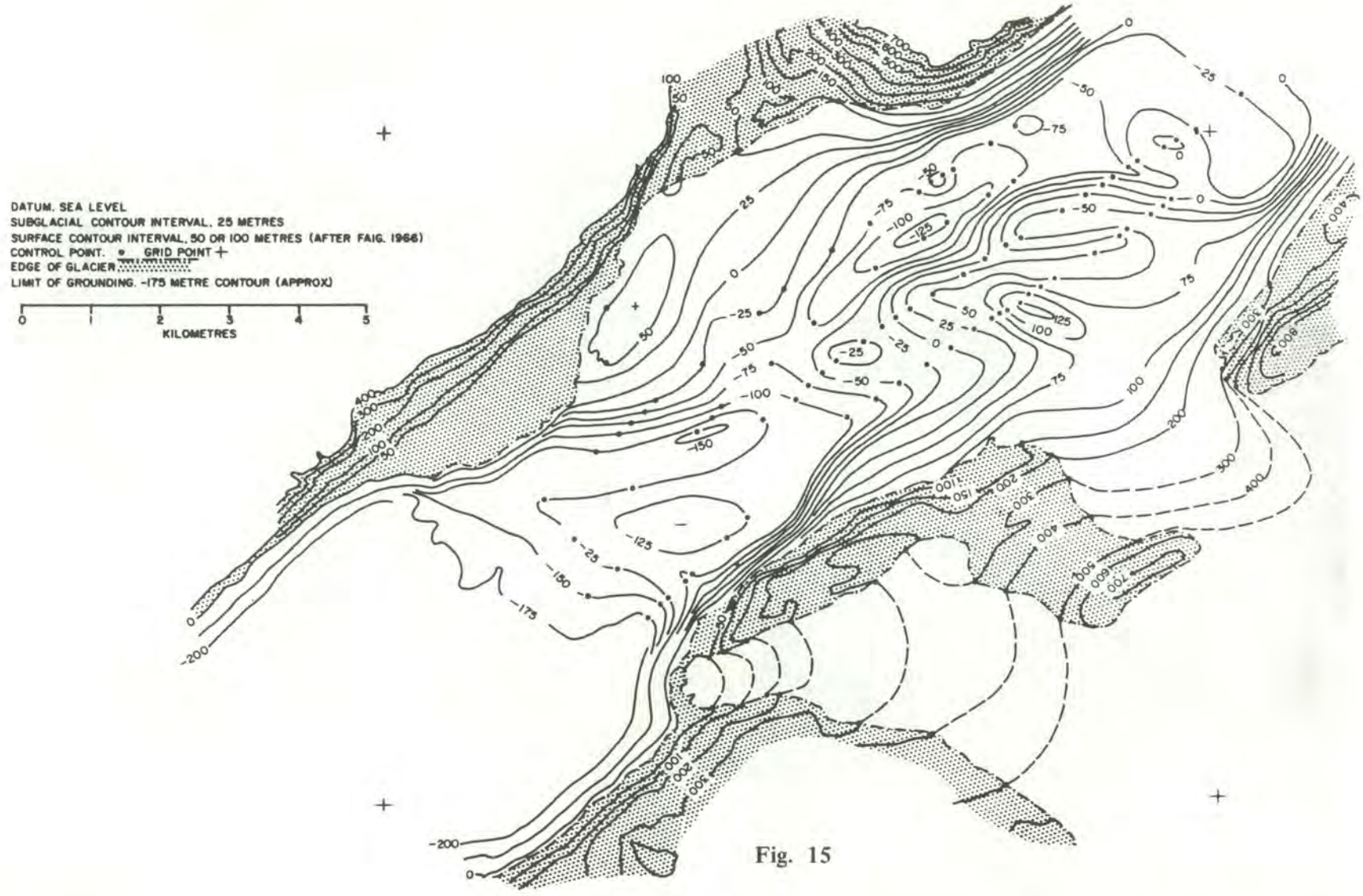
DATUM. SEA LEVEL
SUBGLACIAL CONTOUR INTERVAL, 25 METRES
SURFACE CONTOUR INTERVAL, 50 OR 100 METRES (AFTER FAIG, 1966)
CONTROL POINT. ● GRID POINT +
EDGE OF GLACIER
LIMIT OF GROUNDING. -175 METRE CONTOUR (APPROX)
0 1 2 3 4 5
KILOMETRES

Fig. 15

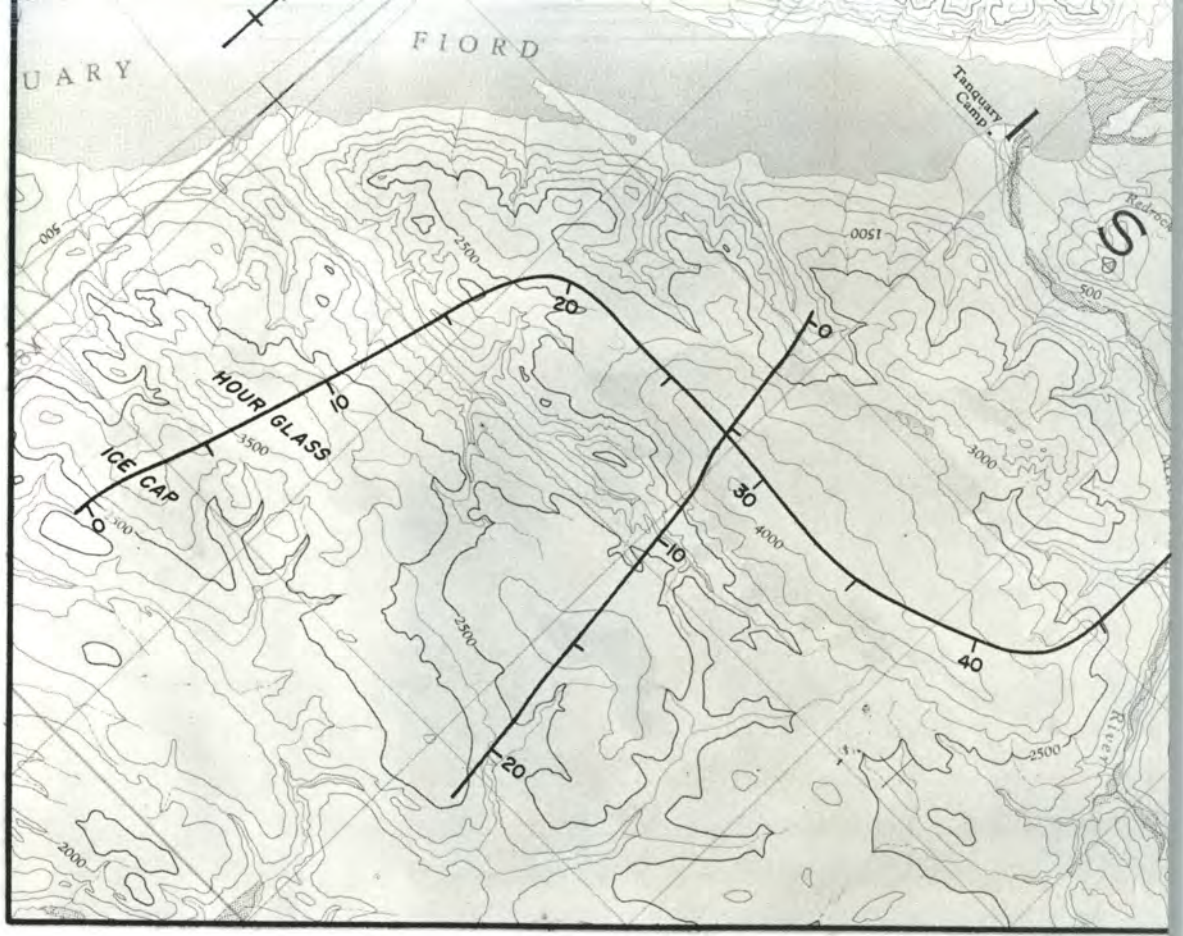
UARY
FIORD
Tanquary Camp
HOUR GLASS
ICE CAP
0
10
20
30
40
500
1500
2500
3500
3000
4000
2000
River

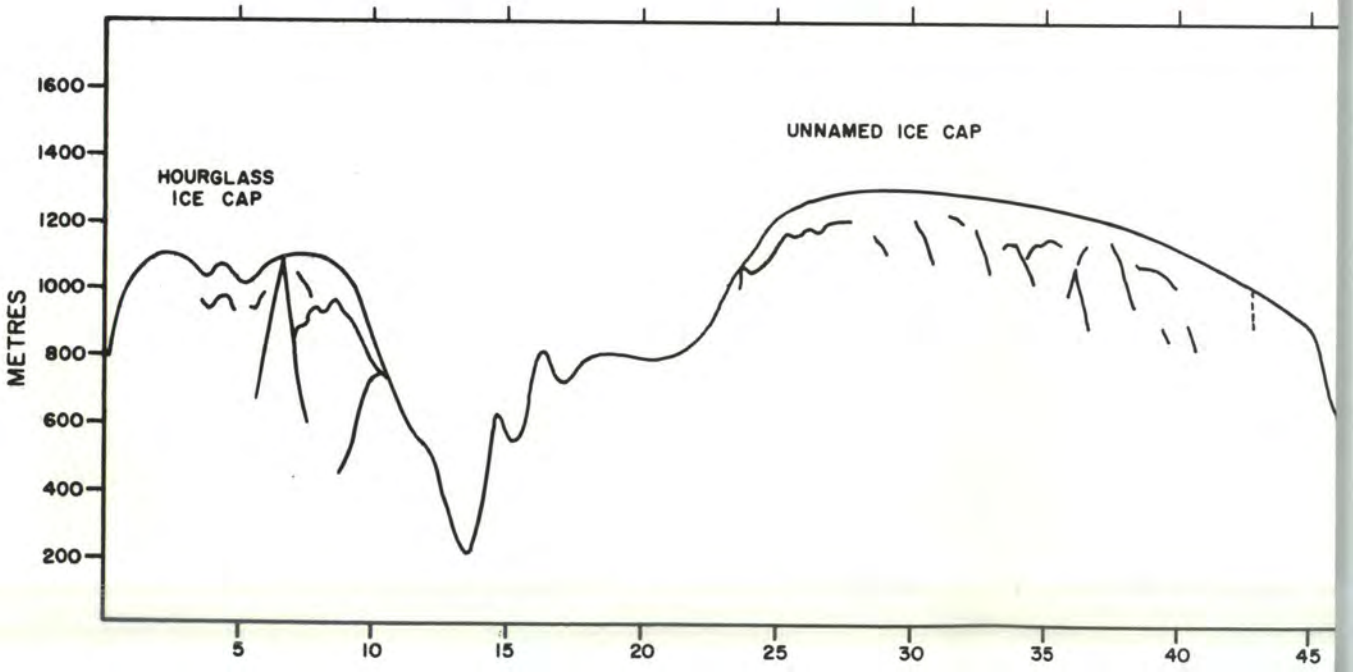
HOURGLASS
ICE CAP
UNNAMED ICE CAP
METRES
1600
1400
1200
1000
800
600
400
200
5
10
15
20
25
30
35
40
45

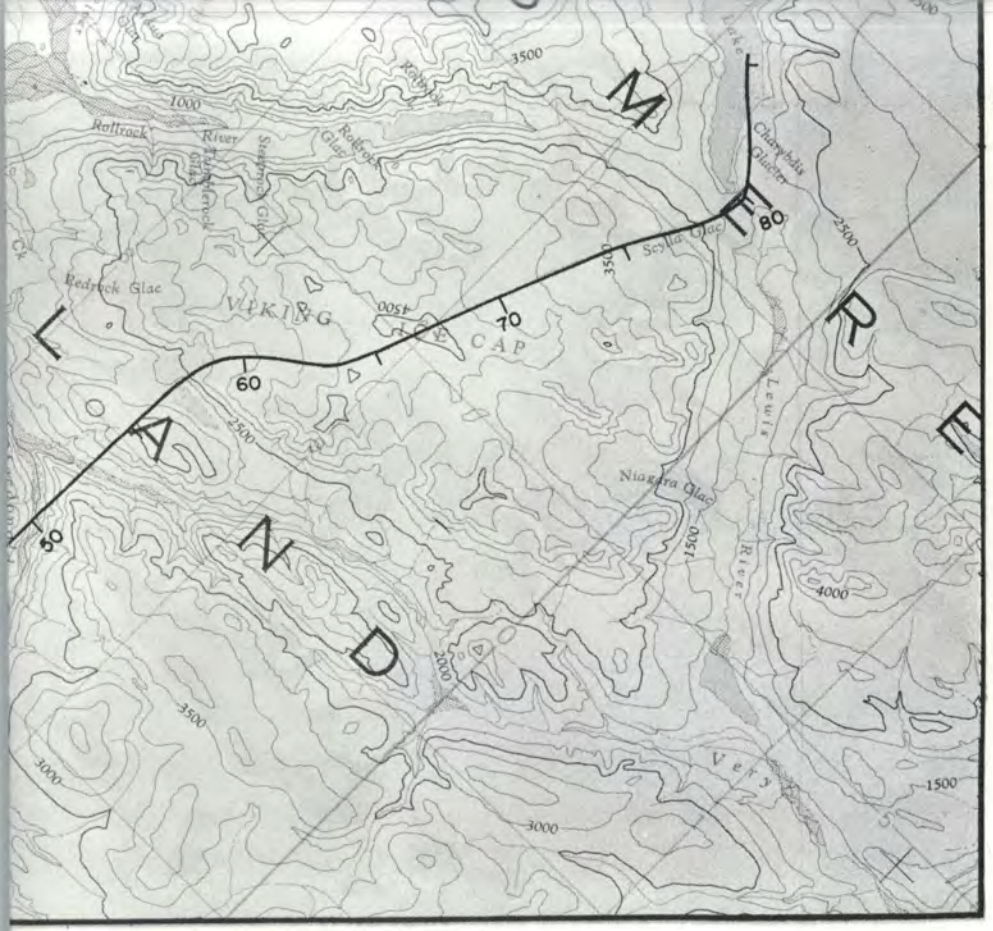

Rollrock
River
Rollrock Glac
Charybdis Glacier
Scylla Glac
Redrock Glac
VIKING ICE CAP
Niagara Glac
Lewis River
Very
50
60
70
80
1000
1500
2000
2500
3000
3500
4000

Fig. 16(a)

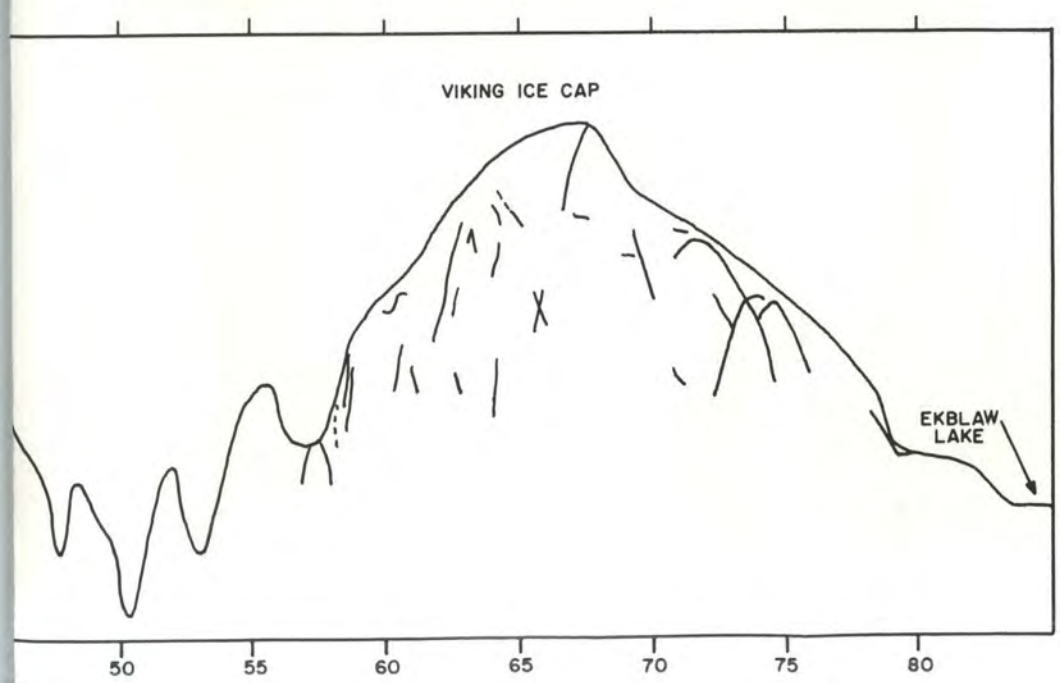

VIKING ICE CAP
EKBLAW LAKE
50
55
60
65
70
75
80

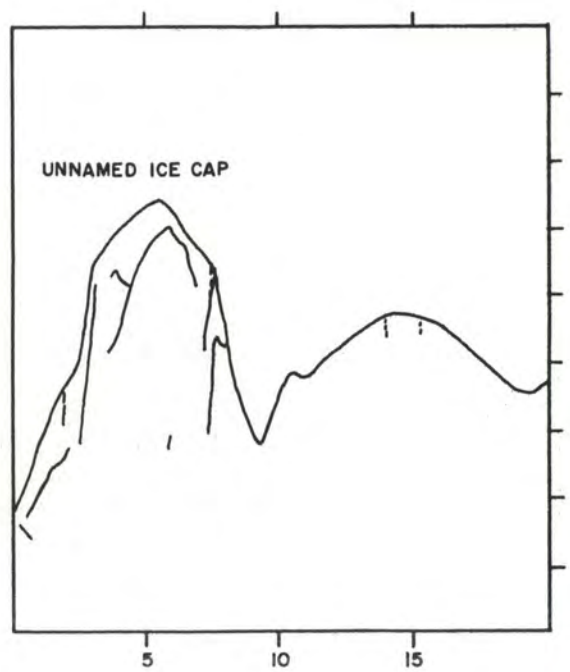

UNNAMED ICE CAP
5
10
15

Fig. 17

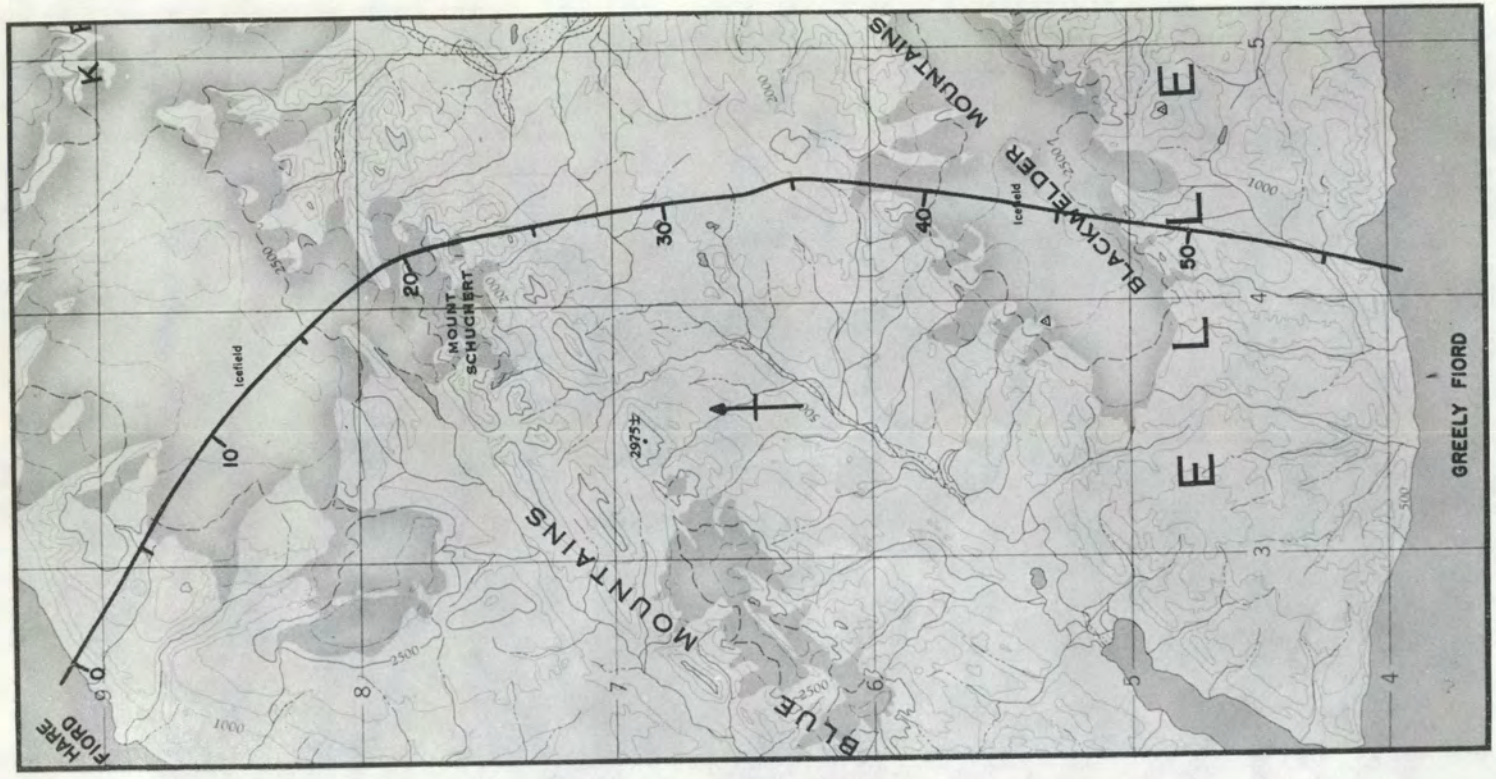

Fig. 18(a)

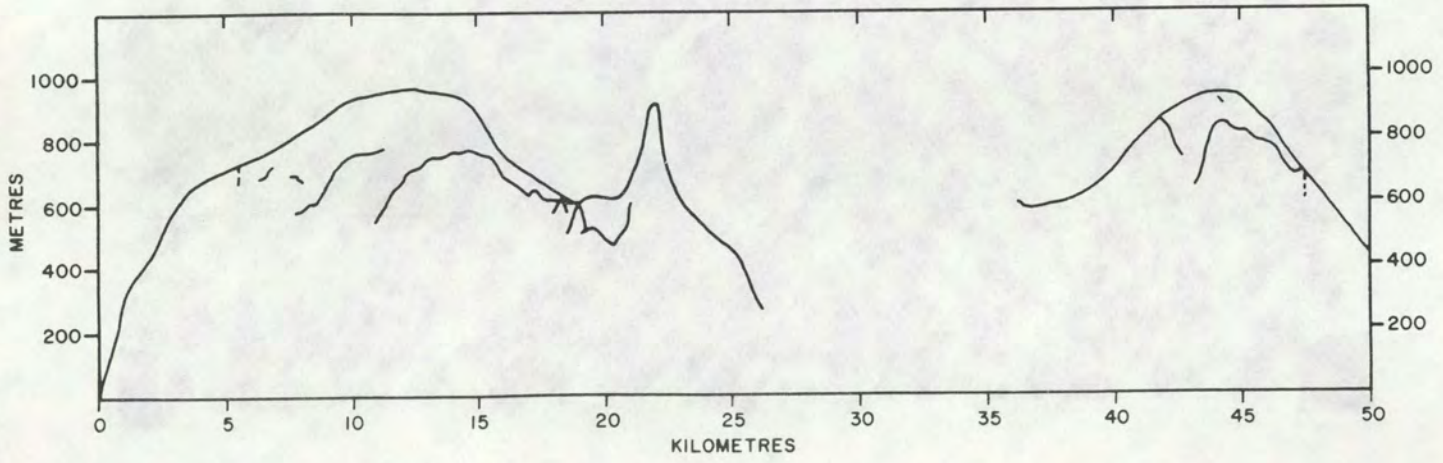

Fig. 18(b)

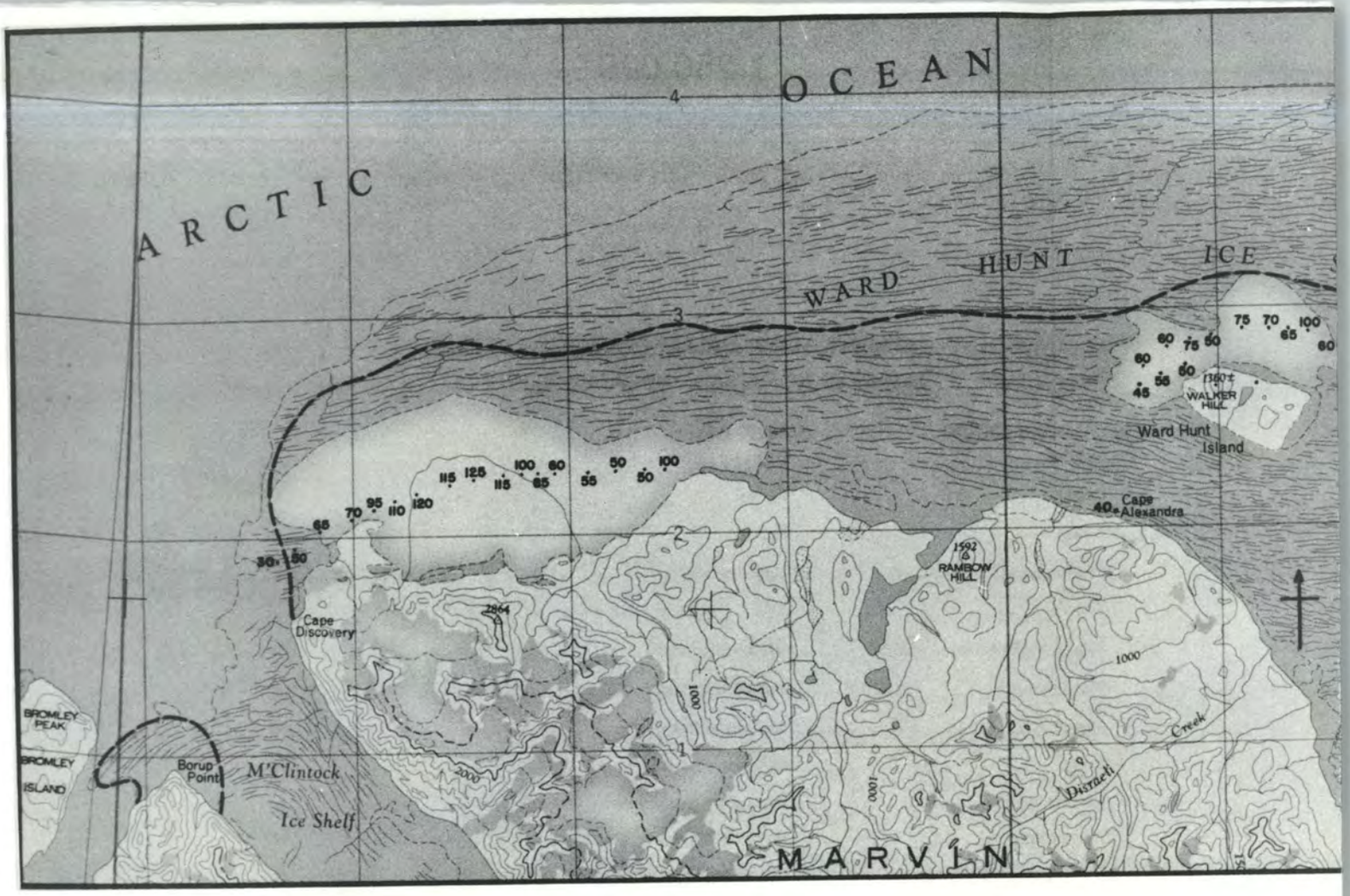

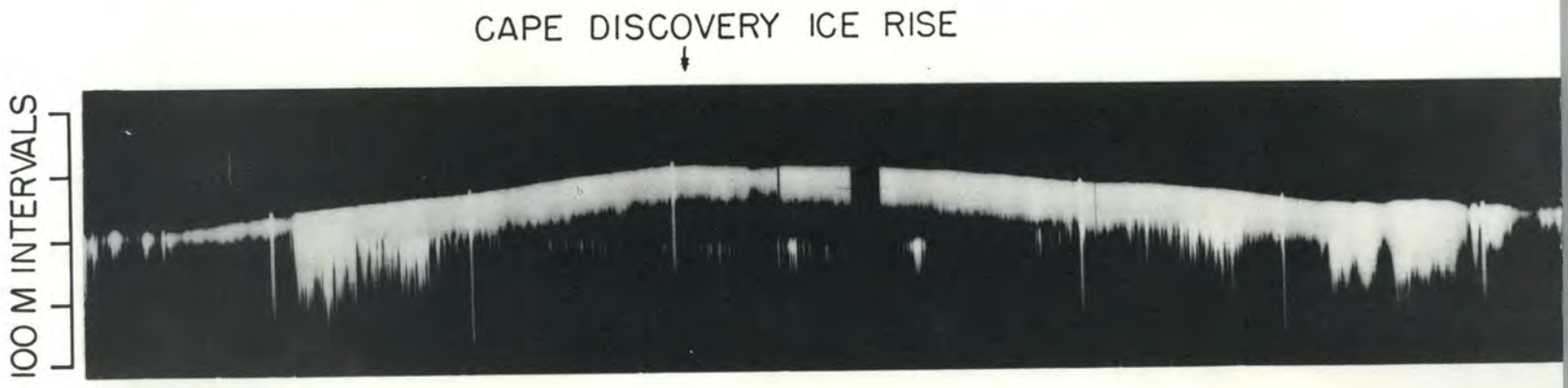

Fig.19(b)

Fig.19(b) contd.

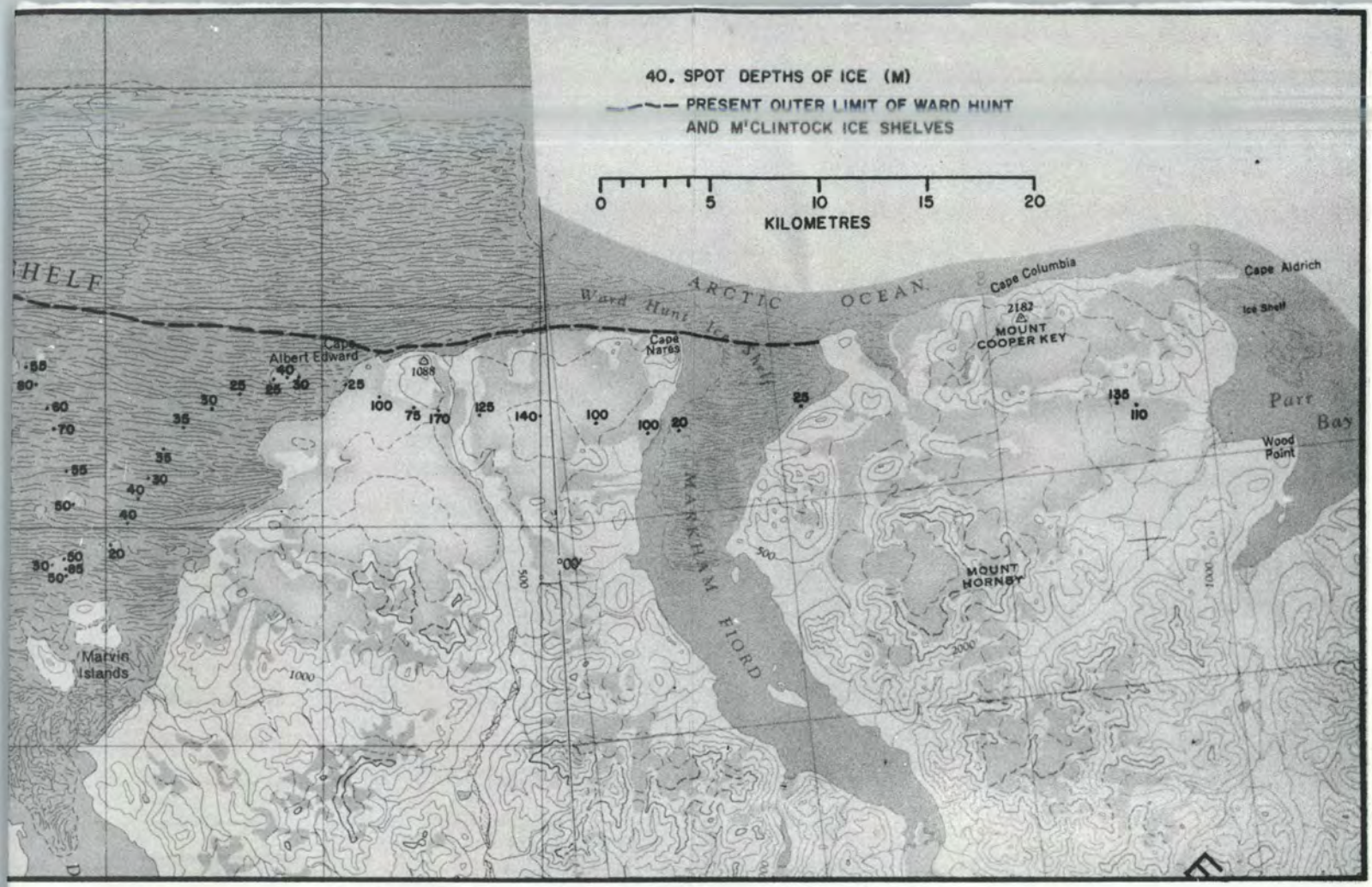

Fig. 19(a)

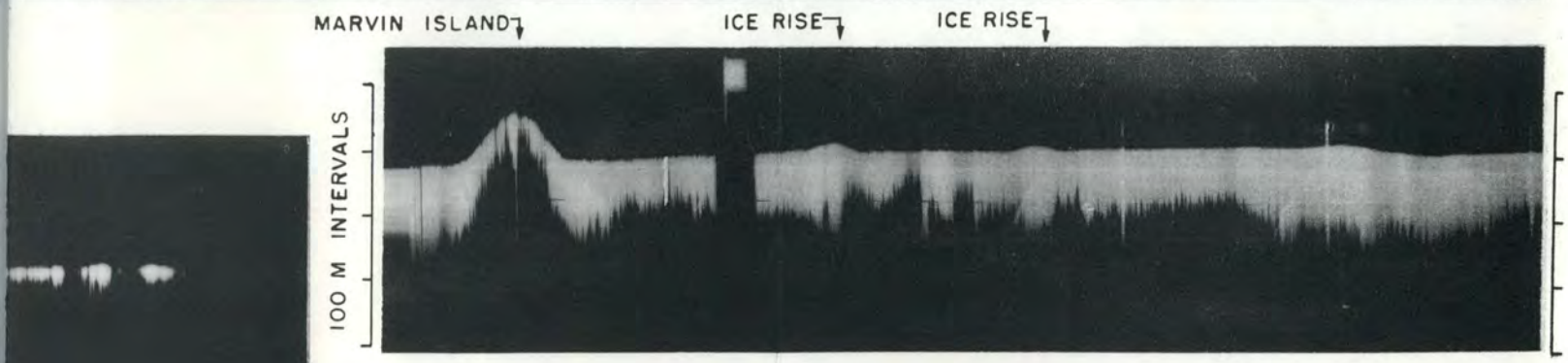
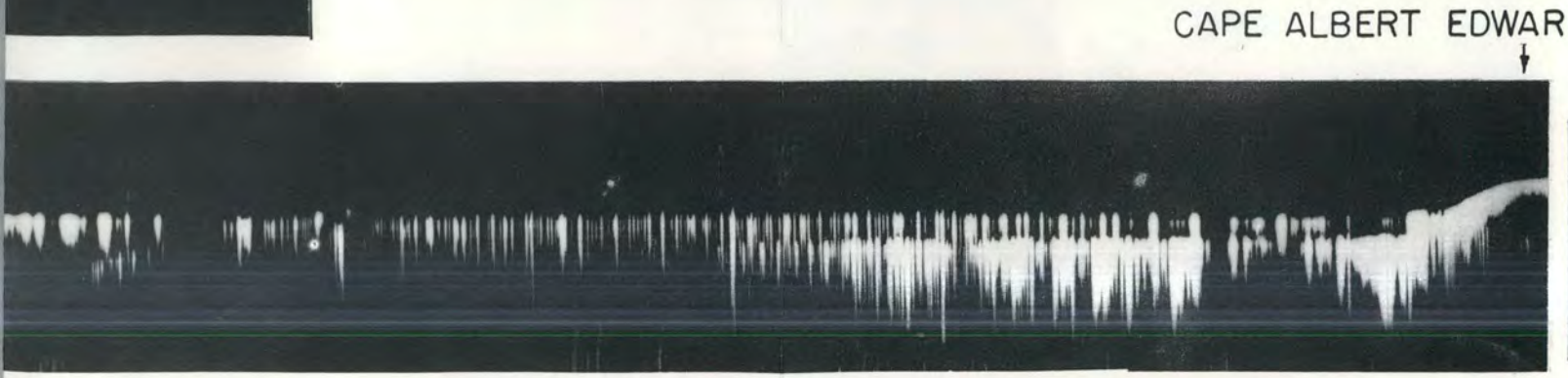
Fig. 19(c)